DETECTION OF HYPOXIA-INDUCIBLE mRNAS IN THE PLASMA OF NON-SMALL CELL LUNG CANCER PATIENTS

MASTER'S THESIS
Institute of Medical Technology
University of Tampere
January 2009
Alise Hyrskyluoto

PRO GRADU -TUTKIELMA

Paikka:	TAMPEREEN YLIOPISTO Lääketieteellinen tiedekunta Lääketieteellisen teknologian instituutti
Tekijä:	HYRSKYLUOTO, ALISE KRISTIINA
Otsikko:	Hypoksian säätelemien lähetti-RNA:iden havaitseminen ei-pienisoluista keuhkosyöpää sairastavien potilaiden plasmasta.
Sivumäärä:	65 sivua
Ohjaajat:	Professori Seppo Parkkila, FT Mika Hilvo
Tarkastajat:	FT Mika Hilvo, Professori Vesa Hytönen
Aika:	Tammikuu 2009

Tiivistelmä

Tutkimuksen tausta ja tavoitteet: Tämän tutkielman tavoitteena oli tutkia hypoksiainduktiofaktori 1 α:n (*HIF-1α*) ja kolmen hypoksian indusoiman geenin, hiilihappoanhydraasi 9 ja 12 (*CA9 ja CA12*) sekä osteopontiinin (*OPN*), lähetti-RNA-molekyylien (l-RNA-molekyylien) ilmentymistä ei-pienisoluista keuhkosyöpää sairastavien potilaiden plasmasta sekä arvioida kyseisten geenien potentiaalia syövän biomarkkereina. Keuhkosyöpä on maailmanlaajuisesti yleisin syöpä ja merkittävin syöpäkuolemien aiheuttaja. Tehokkaita plasman biomarkkereita kliiniseen käyttöön keuhkosyövän seulonnassa ja diagnosoinnissa ei ole vielä saatavilla. Uusien mahdollisten syövän markkereiden löytämisellä olisi positiivinen vaikutus keuhkosyöpäpotilaiden ennusteeseen, sillä niiden avulla syöpä voitaisiin havaita aikaisemmassa vaiheessa.

Tutkimusmenetelmät: *HIF-1α*:n, *CA9*:n, *CA12*:n ja *OPN*:n l-RNA-molekyylien ilmentymistä tutkittiin kvantitatiivisella reaaliaikaisella PCR-menetelmällä (qRT-PCR). Tulosten normalisointiin käytettiin kahta referenssigeeniä, ubikitiini C:tä (*UBC*) ja beta-2-mikroglobuliinia (*B2M*). Veren plasman l-RNA-molekyylien ilmentymistä mitattiin 95 syöpäpotilaan näytteestä ja 24 kontrollinäytteestä. Tuloksista tehtiin tilastolliset analyysit.

Tutkimustulokset: Hiilihappoanhydraasien l-RNA-molekyylien ilmentymisestä ei havaittu plasmanäytteissä. Osteopontiinin, *HIF-1α:n* sekä referenssigeenien osalta saatiin l-RNAn ilmentymistasoja mitattua. Syöpäpotilailla todettiin l-RNAn ilmentymistasojen kohonneen. Tilastollisesti merkittäviä eroja syöpäpotilaiden ja kontrollien välillä löydettiin *UBC:n* ja *OPN:n* osalta. Suurin osa korrelaatiosta plasman l-RNAn ilmentymistasojen sekä kliinisten parametrien tai vern biomarkkereiden välillä eivät olleet tilastollisesti merkittäviä. Myöskään eloonjäämisennusteen analyysi ei osoittanut selvää suhdetta plasman l-RNAn ilmentymistasojen ja syövästä selviytymisen välillä.

Johtopäätökset: qRT-PCR-menetelmän käyttö diagnoosimenetelmänä vaikuttaa haasteelliselta, johtuen plasman nukleiinihappojen alhaisesta ilmentymistasosta. Tässä tutkimuksessa löydettiin tilastollisesti merkittäviä eroja *OPN*:n ja *UBC*:n l-RNAn ilmentymistasoissa syöpäpotilailla ja kontrolleilla, plasman l-RNAn ilmentymistasoilla voikin olla diagnostista merkitystä. Toisaalta testin spesifisyys ja sensitiivisyys olivat alhaisia verrattuna siihen mitä kliinisiltä diagnoosimenetelmiltä vaaditaan.

MASTER'S THESIS

Place:	UNIVERSITY OF TAMPERE Faculty of Medicine Institute of Medical Technology
Author:	HYRSKYLUOTO, ALISE KRISTIINA
Title:	Detection of Hypoxia-inducible mRNAs in the Plasma of Non-Small Cell Lung Cancer Patients
Pages:	65 pages
Supervisors:	Professor Seppo Parkkila, PhD Mika Hilvo
Reviewers:	PhD Mika Hilvo, Professor Vesa Hytönen
Date:	January 2009

Abstract

Background and aims: The aim of this study was to investigate the mRNA expression levels of hypoxia-inducible factor 1α and three hypoxia-inducible genes, *CA9, CA12* and *OPN,* in NSCLC patients' plasma and to evaluate their potential as clinical tumor markers. Lung cancer is one of the most common malignancies in the world and the leading cause of cancer-related deaths. Plasma biomarkers have not yet been available as an effective clinical tool in screening or early diagnosis of lung cancer. The discovery of new potential tumor markers would have positive impact on the clinical outcome of lung cancer patients by helping to detect the disease in an early phase.

Methods: mRNA expression of *HIF-1α, OPN, CA IX* and *CA XII* was studied by quantitative real-time polymerase chain reaction (qRT-PCR). Two house-keeping genes, *B2M* and *UBC*, were used for normalization. mRNA levels were assessed in the 95 blood plasma samples of NSCLC patients and 24 blood plasma samples of healthy volunteers. The qRT-PCR results were statistically analysed.

Results: No significant *CA IX* and *CA XII* expression was found to be detectable in blood plasma samples. Reasonable signals were obtained for *OPN* and *HIF-1α* and two house-keeping genes, *UBC* and *B2M*. Elevated mRNA levels were observed in cancer patients' plasma. Statistically significant difference was found between *UBC* and *OPN* mRNA levels of healthy controls and NSCLC patients. The majority of correlations between mRNA levels and clinical parameters or blood biomarkers were not statistically significant. Neither did the survival analysis show any significant relationship between survival and mRNA levels.

Conclusions: Due to low levels of circulating RNA in plasma quantitative real-time polymerase chain reaction seems to be challenging for routine diagnostics. In this study, a statistically significant difference was found in *UBC* and *OPN* mRNA levels between the healthy controls and NSCLC patients. Therefore, it is possible that the plasma RNA levels have some diagnostic value, although the test specificities and sensitivities remained quite low compared to the requirements set for routine laboratory diagnostics.

CONTENTS

ABBREVATIONS

AC	adenocarcinoma
ACS	American Cancer Society
AP	activator protein (transcription factor)
bHLH	basic helix-loop-helix motif
BTA	bladder tumor antigen
CA	cancer antigen
CA IX	carbonic anhydrase IX
CA XII	carbonic anhydrase XII
CA9	carbonic anhydrase 9 (refers to the human gene)
CA12	carbonic anhydrase 12 (refers to the human gene)
cDNA	complementary deoxyribonucleic acid
CEA	carcinoembryonic antigen
CYFRA	cytokeratin fragment
EGFR	epidermal growth factor receptor
EPO	erythropoietin
FIH-1	factor inhibiting HIF-1
GLUT	glucose transporter
HIF	hypoxia-inducible factor
HRE	hypoxia-response element
IRES	internal ribosome entry site
MAPK	mitogen-associated protein kinase
mRNA	messenger ribonucleic acid
NCI	National Cancer Institute
NF-1	nuclear factor 1
NF-κB	nuclear factor-kappa B
NSCLC	non-small cell lung cancer
NSE	neuron-specific enolase
SCC	squamous cell carcinoma
SCCA	squamous cell carcinoma antigen
SCLC	small cell lung carcinoma
OPN	osteopontin
OPN	osteopontin (refers to the human gene)
PHD	prolyl hydroxylase-domain protein
PSA	prostate-specific antigen
PI3K	phosphatidylinositol 3-kinase
Pro-GRP	pro-gastrin-releasing peptide
VHL	von Hippel-Lindau protein
VEGF	vascular endothelial growth factor
WHO	World Health Organization

1 Introduction

Lung cancer is the most common cause of cancer mortality worldwide. It is responsible for 17.8% of all cancer deaths, exceeding the combined mortality from breast, prostate, and colorectal cancers. Despite recent advances in understanding biology behind lung cancer, the 5-year survival rate for the patients remains poor. Lung cancer is a heterogeneous disease. It has been traditionally diagnosed and classified according to its histologic morphology. (Jamel et al. 2008; Hu et al. 2005) The majority of lung tumors are carcinomas which are divided into two broad categories of small cell carcinoma (SCLC) and non-small cell lung cancer (NSCLC). NSCLC accounts for approximately 85% of all lung cancer cases (Breuer et al. 2005). To improve the curability of lung cancer, there is a need for identification of new specific molecules involved in tumorigenesis and progression. Early detection of lung cancer is challenging, in part because currently used tumor markers have not turned out to be effective tools in screening or early diagnosis of the disease. There is a need for tumor markers, that could reflect the disease activity or predict response to therapy and in this way have a positive impact on the clinical outcome of lung cancer patients. (Niewoehner & Rubins, 2003)

Tumor hypoxia results from an inadequate supply of oxygen that compromises biologic functions. It is strongly associated with tumor propagation, malignant progression, and resistance to therapy and it has thus become a central issue in tumor physiology and cancer treatment. (Höckel & Vaupel, 2001) The effect of hypoxia on malignant progression is mediated by a series of hypoxia induced proteomic and genomic changes which activate angiogenesis, anaerobic metabolism, and other processes that enable tumor cells to survive or escape hypoxic conditions. The hypoxia-inducible factors (HIFs) are major regulators of tumor cells adapting to hypoxic stress. (Vaupel, 2004)

HIF-1 is a transctiption factor composed of two subunits, HIF-1α and HIF-1β. Many hypoxia-inducible genes are controlled by HIF-1. Increased concentrations of HIF-1 in the proteome of hypoxic cells results from increased transcription of *HIF-1α* and *HIF-1β* genes and decreased HIF-1α protein degradation. (Höckel & Vaupel, 2001) The

adaptive responses to hypoxia cause changes in gene expression, mediated by HIFs. (Vaupel, 2004)

Transmembrane carbonic anhydrases CA IX and CA XII are induced by the HIF pathway activated due to genetic defect or physiological hypoxia. CA IX, and possibly CA XII, participates in pH regulation, which is important for survival of hypoxic cells. CA IX and XII are expressed in a broad range of different tumor types and for selected cancers they are potential diagnostic tumor markers. (Wykoff et al. 2000) Another hypoxia-inducible gene, osteopontin, is an extracellular molecule which is involved in tumor development and progression. Osteopontin levels are increased in the circulating plasma of cancer patients hence it may serve as a tumor marker for cancer diagnosis and prognosis. (Hu et al. 2005)

There is a need of novel tumor markers and for development of sensitive and specific non-invasive cancer tests. In this study, the mRNA expression levels of *HIF-1α* and three hypoxia-inducible genes, *CA9, CA12* and *OPN* was assessed in NSCLC patients' plasma by quantitative real-time PCR.

2 Review of the literature

2.1 Lung cancer

Lung cancer is the most common cancer worldwide and the leading cause of cancer-related deaths, for both men and women, in industrialized countries (Bremnes et al. 2005). World Health Organization (WHO) has reported that lung cancer accounts for 1.2 million new cases annually and is responsible for 17.8% of all cancer deaths. Lung cancer alone exceeds the combined mortality from breast, prostate, and colorectal cancers (Bhattacharjee et al. 2001, Jemal et al. 2008). Despite recent improvements in the detection and treatment of lung cancer the 5-year survival rate remains <15%. The overall survival rate remains poor because, in the early stages of disease, lung cancer tends to be asymptomatic and at the time of diagnosis most tumors are overtly or covertly metastatic. (Breuer et al. 2005)

The most significant risk factor for lung cancer is smoking. Approximately 87% of lung cancer cases are smoking-related and the relative risk of developing lung cancer is 24 times higher among smokers than among non-smokers. Passive smoking also increases the risk of developing lung cancer. (Duarte & Paschoal 2005) The contribution of genetic and environmental factors to lung cancer risk is thought to be small compared to smoking but some of them might synergise with smoking (Heighway & Betticher 2004).

Lung cancers have been traditionally diagnosed and classified according to their histologic morphology (Rosell et al. 2004). Lung cancers are generally heterogeneous, consisting frequently of cells of different histological subtypes. The majority of lung tumors are carcinomas which are divided into two broad categories of small cell carcinoma (SCLC) and non-small cell lung cancer (NSCLC) based on clinical behaviour and histological appearance. Other rarer lung tumor types include carcinoids, carcinosarcomas, pulmonary blastomas, and giant and spindle cell carcinomas (Heighway & Betticher 2004). NSCLC accounts for approximately 85% of all lung cancer cases (Breuer et al. 2005).

2.1.1 Non-small cell lung cancer (NSCLC)

Because of the heterogeneous nature of non-small cell lung cancer, even in patients with similar clinical and pathological features, the outcome varies: some are cured, whereas in others, the cancer recurs. Staging system for lung cancer is based on clinical and pathological findings. (Chen et al. 2007)

NSCLC is divided histologically into three main types; squamous cell carcinoma (SCC), adenocarcinoma (AC) and large-cell carcinoma (Breuer et al. 2005). SCC comprises approximately 30% of lung cancers. These tumors tend to arise centrally within the lungs inside a bronchus. AC is the most common type of disease subtype, accounting for about 40% of invasive lesions. Patients with AC tend to have better prognosis than those with other types of lung cancer. AC usually occurs in more peripheral locations arising from the smaller airways but they can be found centrally in the main bronchus. Large-cell carcinoma accounts approximately 10 to 15% of lung cancers. They are undifferentiated tumors which lack the diagnostic features of other subtypes. (Heighway & Betticher 2004)

Pathological analysis have shown that SCC arises after a series of progressive pathological changes in the bronchial epithelium, that appear to represent the intermediate steps in a process in which the cells evolve from a normal phenotype into a malignant phenotype. Transformation of the normal phenotype into malignant phenotype requires accumulation of multiple genetic and epigenetic changes. (Breuer et al. 2005) WHO has categorized these premalignant lesions as squamous metaplasia, mild, moderate and severe dysplasia and carsinoma *in situ*. After these premalignant stages, lung cancer emerges from carcinoma *in situ* to an overt carcinoma. Adenocarcinomas are also thought to develop, at least in part, from premalignant precursor lesions. For AC, atypical adenomatous hyperplasia is the only known candidate precursor lesion. (Breuer et al. 2005; Brambilla et al. 2001)

The biology behind NSCLC has not been well understood, but in recent years with the development of techniques in molecular biology, the understanding of abnormalities in lung cancer cells at a molecular level has increased dramatically. Carcinogenesis of NSCLC requires accumulation of multiple genetic and epigenetic changes, with each

step resulting in some form of growth and/or cellular survival advantage. Changes in this multistep process include proto-oncogene activation, loss of tumor suppressor genes, deregulation of apoptosis and telomerase control, sustained angiogenesis and tissue invasion. (Breuer et al. 2005)

Detailed knowledge about molecular alterations early in the carcinogenic process is valuable. It may provide new tools for pathological sub-classifications with clinically meaningful properties such as prognostic, diagnostic and therapeutic strategies. Molecular studies may reveal genetic profiles that reflect the initiation of malignancy or identify cells that have reached a point of no return in terms of malignant transformation. Several of these alterations can be used as biomarkers for the early detection of lung cancer and risk assessment. (Breuer et al. 2005)

2.2 Tumor markers

2.2.1 General aspects

According to National cancer institute (NCI) tumor markers are substances produced by tumor cells or by other cells of the body in response to cancer or certain benign conditions. Tumor markers can be found in the blood, in the urine, in the tumor tissue, or in other tissues. Different tumor markers are found in different types of cancer, and levels of the same tumor marker can be altered in more than one type of cancer. A tumor marker can also be referred to as a cancer biomarker.

Tumor markers can be used in the detection, diagnosis, and management of some types of cancer. To date, most detection methods identify fully developed cancer, not the pre-malignant or early lesions amenable to resection and cure. (Manne et al. 2005)

Although an abnormal tumor marker level may suggest cancer, this alone is usually not enough to diagnose cancer. To date only about dozen substances which seem to be expressed abnormally when some types of cancer are present, have been identified and clinically used. Some of these substances are also found in other conditions and diseases. An ideal tumor marker would have 100% sensitivity and specificity, this

means that everyone with cancer would have a positive test result and everyone without cancer would have a negative test result. In other worlds sensitivity is used to describe the probability of a positive test among patients with disease, and specificity is used to describe the probability of a negative test among patients without disease. None of the currently used tumor markers achieve 100% sensitivity and specificity. Therefore panels of tumor markers, rather than single tumor marker, seem to be a promising alternative for the clinical use. (Manne et al. 2005)

2.2.2 Different types of tumor markers

Tumor markers were first thought to be useful in screening and diagnosing cancer in an early phase of the disease. Unfortunately, very few tumor markers have been shown to be helpful in this way. The only tumor marker widely used in screening is the prostate-specific antigen (PSA) blood test, which is used to screen for prostate cancer (ACS 2007). The prostate-specific antigen (PSA) has high sensitivity (greater than 90%) but low specificity (~25%) (Manne et al. 2005).

Only a small fraction of tumor markers that have been discovered or declared are in clinical use (Manne et al. 2005). Some examples of the commonly used tumor markers are represented in table 1. These markers are used mainly in patients who have already been diagnosed with cancer to monitor their response to treatment or detect the return of cancer after treatment.

Tumor markers can be divided into the following categories, based on their utility:
1) Screening and early detection – if used for finding cancer at an early stage.
2) Diagnostic – if used to assess the presence or absence of cancer.
3) Prognostic – if used to assess the survival probabilities of patients or to detect the aggressive phenotype and determine how the cancer will behave.
4) Predictive – if used to predict whether different therapies will be effective, or to monitor the effectiveness of treatment.
5) Target – if used to identify the molecular targets of novel therapies and which molecular markers expression were affected by therapy. (Manne et al. 2005)

Table 1. Some commonly used tumor markers. (Data adapted from American Cancer Society 2007 and Manne et al. 2005)

Tumor marker	Cancer types	Application
alpha-fetoprotein (AFP)	liver cancer (hepatocellular carcinoma), testicular cancers	help diagnose, monitor treatment, and determine recurrence
bladder tumor antigen (BTA)	bladder cancer	help diagnose and determine recurrence
cancer antigen 15-3 (CA 15-3)	breast cancer, and others including lung and ovarian cancers	stage disease, monitor treatment, and determine recurrence
cancer antigen 27.29 (CA 27.29)	breast cancer	monitor tratment
cancer antigen 72-4 (CA 72-4)	ovarian and pancreatic cancer and cancers starting in the digestive tract	studies of this marker are still in progress
cancer antigen 125 (CA 125)	epithelial ovarian cancer	help diagnose, monitor treatment, and determine recurrence
cancer antigen 19-9 (CA 19-9)	pancreatic, sometimes colorectal cancer and cancer of stomach and bile ducts	stage disease, monitor treatment, and determine recurrence
carcinoembryonic antigen (CEA)	colorectal, lung, breast, thyroid, pancreatic, liver, cervix, and bladder	monitor treatment and determine recurrence
HER1 (EGFR)	solid tumors, such as of the lung (non small cell), head and neck, colon, pancreas, or breast	guide treatment and determine prognosis
neuron-specific enolase (NSE)	neuroblastoma, small cell lung cancer	monitor treatment
prostate-specific antigen (PSA)	prostate cancer	screen for and help diagnose, monitor treatment, and determine recurrence

2.2.3 Tumor markers in lung cancer

Lung cancer, predominantly NSCLC, is the most fatal cancer worldwide. The relapse rate among patients with an early-stage NSCLC is 40% within 5 years after treatment. The current staging system for NSCLC is inadequate for predicting the outcome of the treatment. (Chen et al. 2007)

The prognosis for lung cancer depends greatly on how early the condition is discovered. If the cancer is treated in its earliest stages, about half of all patients survive at least five years after initial diagnosis. The problem is that only 15% of lung cancers are found in an early stage. (ACS, 2007) Early detection of lung cancer is challenging, in part because currently used biomarkers have not turned out to be effective tools in screening or early diagnosis of the disease (Niewoehner & Rubins, 2003). There is a need for novel tumor markers, that could reflect the disease activity or predict/monitor response to therapy and in this way have a positive impact on the clinical outcome of lung cancer patients.

Tumor markers for lung cancer can be categorically classified into serum biomarkers, tissue biomarkers, and sputum biomarkers (Strauss & Skarin, 1994). Serum biomarkers for lung cancer stand out as being most attractive because of their easy accessibility and the large amount of information they embody outside the primary tumor site in the lung. Serum biomarkers have been studied in hope of achieving early detection of the disease. Nonetheless their clinical usefulness still remains limited at present. (Bharti et al. 2007)

Neuron-specific enolase (NSE) and pro-gastrin-releasing peptide (Pro-GRP) have been used as biomarkers in small-cell lung cancer. In NSCLC, CEA, SCCA, and CYFRA 21-1 are commonly used for screening, and at least one marker among CEA, SCCA and CYFRA is positive in approximately 70% of patients with NSCLC. According to the histological category, the positive rates of CEA and CYFRA are high in patients with adenocarcinoma, and positive rates of CYFRA and SCCA are high in patients with SCC. (Miura et al. 2006)

2.3 Tumor hypoxia

Tumor hypoxia, a reduction in the normal level of tissue oxygen tension, is a common feature of many cancers. Hypoxia in tumors arises as a result of insufficiencies and improper functioning of the tumor vasculature. Hypoxia is toxic to both malignant and normal cells, but cancer cells are able to undergo adaptive changes that allow them to survive and proliferate in a hypoxic environment. These adaptive responses contribute to the malignant phenotype and aggressive behaviour of the tumor. (Harris, 2002)

Tumor hypoxia was first demonstrated by Thomlinson and Gray in 1955 (Thomlinson & Gray, 1955). They reported that human tumors could grow as cords around blood vessels. Tumor cells that located ~150–200 µm away from blood vessels were observed to necrose. This distance is similar to the calculated distance that oxygen diffuses as it passes from the capillary to cells before it is completely metabolized. This limit in oxygen diffusion gives rise to what has been termed as "chronic hypoxia". In this model, the continued proliferation of tumor cells adjacent to blood vessels slowly pushes cells through the oxygen gradient and eventually into necrosis. (Harris, 2002)

Hypoxia can also arise through transient changes in blood flow. These changes include the shut down of aberrant blood vessels, which can also cause blood flow to be reversed. Closed vessels can be reopened, leading to reperfusion of hypoxic tissue with oxygenated blood. This leads to an increase in free-radical concentrations, tissue damage and activation of stress-response genes. This type of hypoxia is known as "acute" or "perfusion-limited" hypoxia. (Wouters et al. 2005)

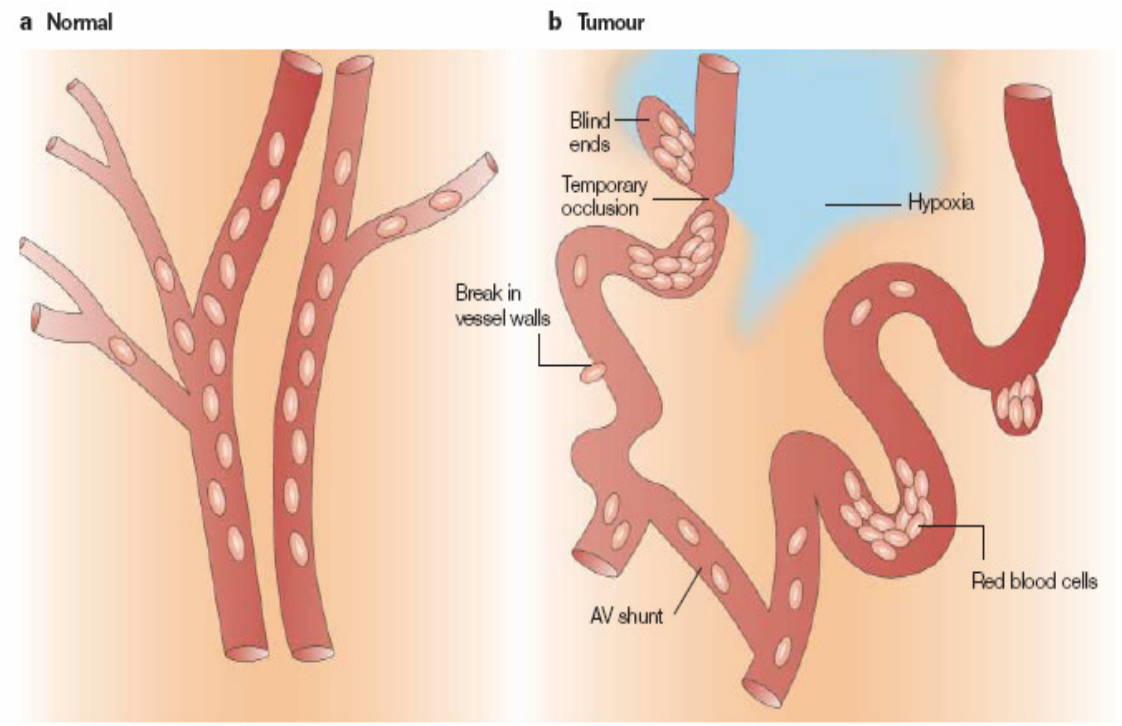

Figure 1. The vascular network of normal tissue versus tumor tissue. Tumors contain regions of hypoxia because their vasculature cannot supply oxygen to all cells. Normal vasculature **(a)** is hierarchically organized, with vessels that are sufficiently close to ensure adequate oxygen supply to all cells, whereas tumor vessels **(b)** are chaotic, tortuous and are often far apart and have sluggish blood flow. The figure is from (Brown & Wilson, 2004)

Progression of an acute hypoxia by temporary obstruction or variable blood flow is illustrated in figure 1. (Brown & Wilson, 2004)

Hypoxia gives selective advantage to more aggressive tumor cells hence it is associated with a more metastatic phenotype in human cancers, thereby compromising curability of tumors by surgery. The cells in hypoxic regions are resistant to both radiotherapy and chemotherapy. Hypoxia has a key role in tumor prognosis, both because it causes resistance to cancer therapies, and because it promotes a more malignant phenotype, by affecting genomic stability, apoptosis, angiogenesis and metastasis. Hypoxia predicts a poor treatment outcome regardless of how the tumors are treated, indicating that it might be an important therapeutic target. (Brown & Wilson, 2004; Wouters et al. 2004)

Hypoxia is highly heterogeneous within the tumor. It has been suggested by Wouters et al. that adaptation to hypoxia during tumor development provides a selective advantage to the tumor by promoting heterogeneity. (Wouters et al. 2004)

Cells undergo a variety of biological changes in response to adapt to hypoxic conditions. Mechanisms that contribute to adaptation of tumor cells to hypoxia can be divided into three distinct pathways. The first is the inhibition or loss of pathways that promote apoptosis in response to hypoxia. The second mechanism which contributes to hypoxia tolerance is the rapid and sustained inhibition of mRNA translation. The third general mechanism of adaptation is the activation of a conserved program mediated mainly by the hypoxia-inducible factors, HIFs. (Wouters et al. 2005)

2.3.1 Hypoxia-inducible factors (HIFs)

Hypoxia-inducible factors mediate the activation of a conserved transcriptional program that assists cells to adapt to hypoxia. This family of oxygen-sensitive transcription factors contains three members; HIF-1, HIF-2 and HIF-3. HIF-1 is the most studied of the group but accumulating information is available concerning HIF-2 and its specificity in gene induction compared to HIF-1. HIF-3 is not as well studied as the other two HIFs. (Wouters et al. 2005) HIF-2 isoform is closely related to HIF-1, and both are able to interact with hypoxia response elements (HRE) to upregulate transcriptional activity.

HIF-2 appears to have a more specialised physiological role than HIF-1 (Maxwell, 2005). HIF-3 is involved in downregulation of the hypoxic response via an alternatively spliced transcription factor, which may function as an inhibitor of HIF-1α. (Makino et al. 2002; Quintero et al. 2004)

2.3.2 Hypoxia-inducible factor 1 (HIF-1)

Semenza and Wang identified the HIF-1 transcription factor in 1992. HIF-1 was discovered by the identification of a hypoxia response element in the enhancer of the human erythropoietin gene. Erythropoietin (EPO) is a hormone that stimulates erythrocyte proliferation and undergoes hypoxia induced transcription. (Semenza & Wang, 1992)

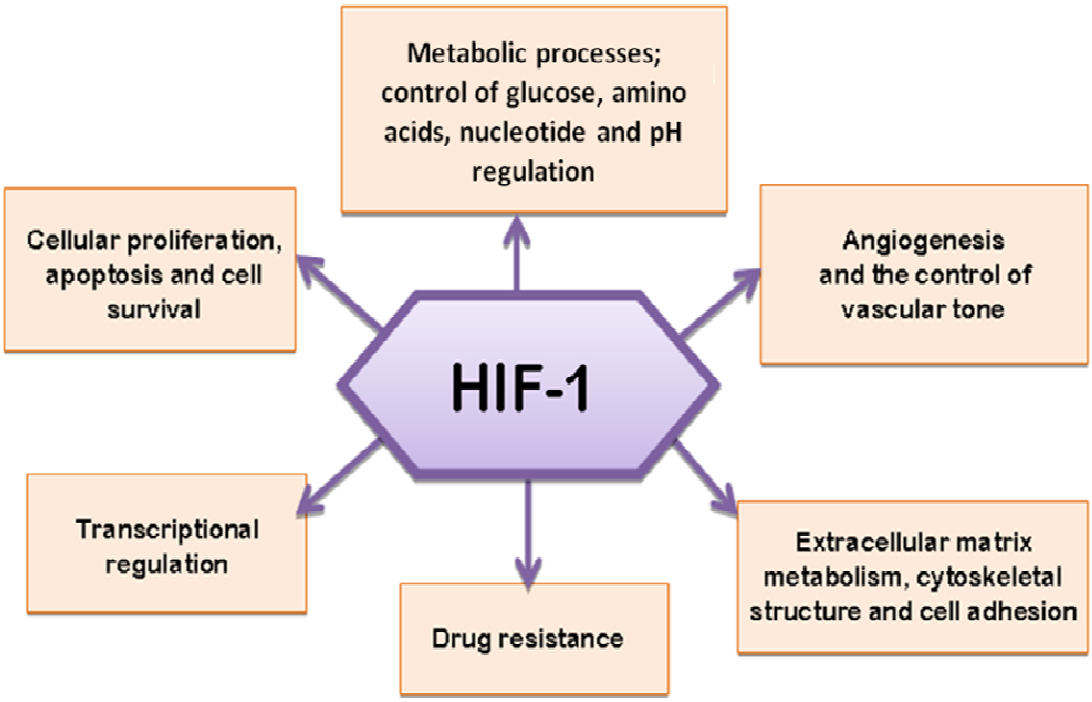

Figure 2. Processes and gene groups that are transcriptionally activated by HIF-1. Figure is drawn on the basis of (Quintero et al. 2004).

Since its discovery, more than 60 putative direct HIF-1 target genes have been identified. These HIF-1 target genes are involved in various biological processes which influence tumor growth, metastasis, and metabolic adaptation. The battery of target genes varies greatly from one cell type to another hence the complete HIF-1 transcriptome is more likely to include rather thousands of genes than hundreds of genes. (Semenza, 2007) Simplified representation of the processes influenced by HIF-1 is represented in figure 2.

2.3.3 HIF-1 – structure and function

HIF-1 is only active as heterodimer. It consists of α and β subunits which both are helix-loop-helix transcription factors. The β-subunit is constitutively expressed and its activity is controlled in an oxygen independent manner. Expression of the α-subunit is induced by cellular hypoxia and is maintained at low levels in most cells with normal oxygen tension. HIF-1α levels must be induced for the HIF-1 transcriptional complex to be functional. The induction of HIF-1α is a critical step in the hypoxic response and it occurs via increased mRNA expression, protein stabilisation, and nuclear localization. (Quintero et al. 2004)

The human HIF-1α gene is located on chromosome 14 whereas the HIF-1β is located on chromosome 1. HIF-1α and HIF-1β are relatively large proteins, being comprised of 826 and 789 amino acids, respectively. Both proteins contain nuclear localization signals and a basic helix-loop-helix motif (bHLH). The basic domain is essential for DNA binding while the HLH domain is responsible for the dimerization of the subunits. Another common feature of HIF-1α and HIF-1β is the PAS (Per-ARNT-Sim) domain. (Déry et al. 2005)

HIF-1α has also some unique features including the oxygen-dependent degradation domain. This domain is highly oxygen-regulated. During normoxia the specific degradation of HIF-1α is triggered through this domain. HIF-1α also contains two transactivation domains which are responsible for the transcriptional regulation of HIF-1 target genes. These domains are also involved in the binding of co-activators which are required for HIF-1's transcriptional activation. The structures of the two HIF-1 subunits are fairly similar but the striking differences in oxygen sensitivity and transactivation ability evidently identify HIF-1α as the main functional protein of the HIF-1 complex. (Déry et al. 2005)

2.3.4 The HIF-1 pathway

HIF-1β is constitutively expressed and its mRNA expression and protein level are maintained at constant levels regardless of oxygen availability, while HIF-1α is an extremely labile protein during normoxia and it has a short half-life ($t_{1/2}$ ~5 min). The

transcription and synthesis of HIF-1α are constitutive and seem not to be affected by oxygen level, while the protein is rapidly degraded during normoxia. Degradation of HIF-1α is triggered by binding of the von Hippel-Lindau tumor-suppressor protein (pVHL). (Semenza, 2007) In the presence of oxygen HIF-1α is bound to the pVHL, which causes HIF-1α to become ubiquitylated and targeted to the proteasome, where it is degraded (Harris, 2002).

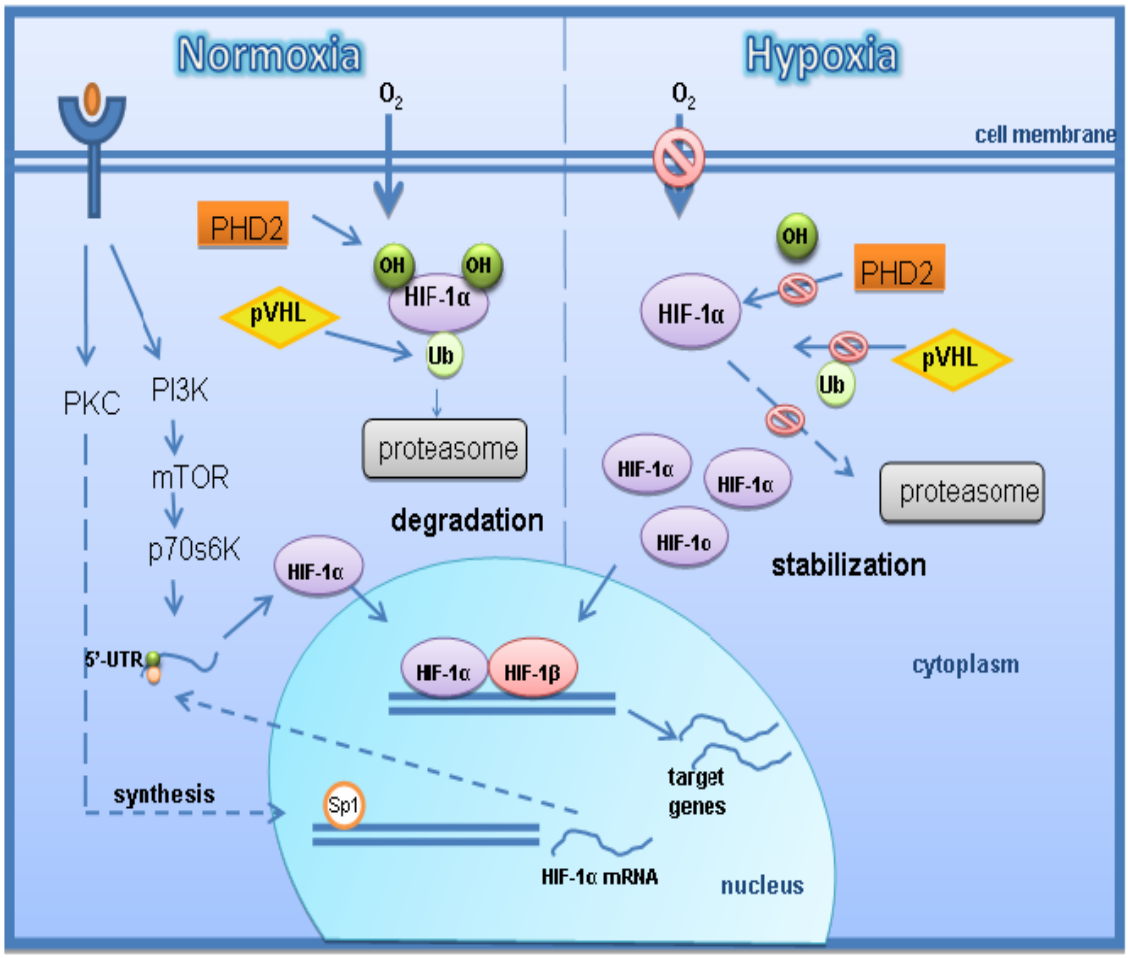

Figure 3. In normal oxygen conditions HIF-1α is hydroxylated, ubiquitinated by the pVHL complex and rapidly targeted to degradation by the proteasome. Most non-hypoxic stimuli activate the PKC and PI3K pathways, which mediate the increased HIF-1α translation. In contrast, under hypoxic conditions, HIF-1α is stabilized, which permits the transcription of genes essential to an adaptive response to hypoxia. Figure is drawn on the basis of (Déry et al. 2005).

Under hypoxic conditions HIF-1α becomes stabilized. When the degradation is inhibited, the HIF-1α protein accumulates and translocates from the cytoplasm to the nucleus, where it dimerizes with HIF-1β, and the HIF complex becomes

transcriptionally active. The HIF complex binds to cis-acting hypoxia response elements (HREs) in the promoter region of its target genes, and recruits co-activator proteins, which leads to increased transcription. (Wang et al., 1995; Semenza, 2007)

The HIF-1α gene is mainly expressed through the action of the Sp1 transcription factor. The promoter region of HIF-1α gene also has other binding sites for transcription factors such as AP-1, AP-2, NF-1 and NF-KB. (Déry et al. 2005) Effective protein translation of HIF-1α during hypoxia is maintained by the presence of an internal ribosome entry site (IRES) located in the 5'-untranslated regions (5'-UTR) of the HIF-1α gene (Lang et al. 2002). Therefore, as mentioned above, transcription and translation levels of HIF-1α are not affected by the switch from normoxia to hypoxia. (Déry et al. 2005)

During normoxia, HIF-1α is hydroxylated on specific residues, ubiquitinated and degraded by the proteasome. Three prolyl-4-hydroxylases, (PHDs 1-3), hydroxylate the proline(Pro)-402 and Pro-564 residues of HIF-1α. The PHDs use molecular O_2, iron and 2-oxoglutarate (α-ketoglutarate) as substrates while generating CO_2 and succinate as by-products. Although overexpression of PHD1, PHD2 or PHD3 results in increased HIF-1α degradation, only PHD2 loss-of-function results the accumulation of HIF-1α in normoxic cells. (Déry et al. 2005; Semenza, 2007) Hydroxylation of proline residues is required for interaction of HIF-1α with the pVHL tumor-suppressor protein. pVHL is the recognition component of an E3 ubiquitin-protein ligase that targets HIF-1α for proteasomal degradation. (Semenza, 2003) Additionally to pVHL recognition, lysine acetylation of HIF-1α also targets HIF-1α for degradation by the proteasome. Under hypoxic conditions, prolyl hydroxylation of HIF-1α is blocked and lysine acetylation is downregulated which allows HIF-1α protein stabilization. (Déry et al. 2005)

Hydroxylation also participates in HIF-1α activation. Factor inhibiting HIF-1 (FIH-1) is an α-ketoglutarate-dependent dioxygenase that hydroxylates aspargine residue, Asn^{803}. FIH inhibits the interaction of HIF-1α with the co-activators p300 and CBP. This hydroxylation is also dependent on oxygen availability, demonstrating the strict regulation of HIF-1 in the presence of oxygen. A subset of genes regulated by HIF-1 appears to be sensitive to O_2-dependent regulation by FIH-1. (Semenza, 2007)

There have been several studies demonstrating that stimulation of different cell types with growth factors (Richard et al. 2000), cytokines (Metzen et al. 1999) and hormones (Corlach et al. 2001) can also lead to the induction and activation of HIF-1 during normoxia. Whereas hypoxia increases HIF-1α levels in all cell types, growth factors and other signalling molecules induce HIF-1α expression in a cell-type-specific manner. Also contrary to hypoxia, stabilization of HIF-1α does not seem to play a role in this non-hypoxic induction of HIF-1. The main mechanism of the non-hypoxic induction is an increase in HIF-1α protein translation. The increase in protein translation alone appears sufficient to shift the balance between synthesis and degradation towards an accumulation of HIF-1α. The phosphatidylinositol 3-kinase (PI3K) pathway and its downstream mediators of many tyrosine kinase signalling pathways, mediate the increased HIF-1α translation. This mechanism involves the activation of the ribosomal s6 protein by the PI3K/p70S6K/mTOR pathway. p70S6K regulates the translation of a group of mRNAs possessing a 5'-terminal oligopyrimidine tract; a stretch of 4-14 pyrimidines found at the extreme 5'-terminus of certain mRNAs. The 5'-UTR of HIF-1α contains these tracts including a long conserved sequence in the extreme 5'-terminus. (Déry et al. 2005) Growth factors, cytokines and oncogenes also stimulate the p42/p44 mitogen-associated protein kinase (MAPK) pathway, which increases HIF-1α activity. It is not surprising, that the pathways that induce HIF-1α, also transduce proliferative and survival signals from growth factor receptors. The concomitant induction of angiogenesis and glycolysis during cell proliferation is mediated partly by activating HIF-1. (Semenza, 2003; Déry et al. 2005) The regulation of HIF-1 during normoxia and hypoxia is summarized in figure 3.

2.3.5 HIF-1 in cancer

HIF-1α overexpression has been demonstrated in several cancer types by immunohistochemical analysis including cancer of the lung (Giatromanolaki et al. 2001), breast (Schindl et al. 2002) and cervix (Birner et al. 2000). In most cancers HIF-1 overexpression is associated with increased mortality (Harris, 2002). HIF-1α is overexpressed in human cancers as a result of intratumoral hypoxia as well as genetic alterations, such as gain-of-function mutations in oncogenes and loss-of-function mutations in tumor-suppressor genes. (Semenza, 2003)

Under hypoxic conditions HIF-1 regulates the transcription of hundreds of genes. Four groups of direct HIF-1 target genes that are relevant to cancer, encode angiogenic factors, glucose transporters and glycolytic enzymes, survival factors and invasion factors. The products of the genes that HIF-1 regulates act at several steps in each of these processes. (Semenza, 2007) Many of the known oncogenic signalling pathways overlap with hypoxia-induced pathways. Expression profiling studies have highlighted many of the genes that are up-regulated by hypoxia through activation of HIF-1.

The most well-studied HIF-1α activated growth factors regulate endothelial-cell proliferation and blood-vessel formation. HIF-1 activates transcription of VEGF and one of its receptors, VEGF receptor 1. VEGF is an angiogenic factor that is secreted by cancer cells and normal cells in response to hypoxia. Its receptors are primarily expressed on endothelial cells. VEGF promotes angiogenesis, glucose transporters 1 and 3 (GLUT1, GLUT3), which activate glucose transport; lactate dehydrogenase (LDH-A), which is involved in the glycolytic pathway and previously mentioned erythropoietin (EPO), which induces erythropoiesis. (Harris, 2002)

Hypoxia can induce programmed cell death both in normal and in neoplastic cells. p53 accumulates under hypoxic conditions through a HIF-1α-dependent mechanism and induces apoptosis. Transcriptional activation of p53 by HIF-1α leads to transcription of many pro-apoptotic proteins. BAD and BAX are both pro-apoptotic proteins that function at the mitochondrial membrane and promote cytochrome c release. Cytosolic cytochrome c interacts with the APAF-1, which activates procaspase-9 conversion to caspase-9. Caspase-9 then activates caspase-3 leading to apoptosis. However, hypoxia also initiates p53-independent apoptosis pathways including those involving genes of the BCL-2 family. Below a critical energy state, hypoxia may result in necrotic cell death. Hypoxia-induced proteome changes leading to cell cycle arrest, differentiation, apoptosis, and necrosis, may explain delayed recurrences, dormant micrometastases, and growth retardation which can occur in large tumors. (Harris, 2002; Vaupel & Mayer, 2007)

Under hypoxic conditions the aerobic metabolism is shut down. Cells adapt to hypoxia by switching the glucose metabolism from the oxygen-dependent tricarboxylic acid cycle and oxidative phosphorylation to glycolysis, the oxygen-independent metabolic

pathway. During hypoxia cells use glycolysis as a primary mechanism of ATP production. HIF-1 has been shown to regulate expression of all the enzymes in the glycolytic pathway, as well as the expression of the glucose transporters. The intermediary metabolites of the glycolytic pathway provide the precursors for synthesis of glycine, serine, purines, pyrimidines and phospholipids, all of which are essential for cell growth and maintenance of cells under stress. (Harris, 2002)

Changes in the metabolic activities of cancer cells affect the overall pH of tumors. An acidic extracellular pH is a fundamental property of the malignant phenotype and it has been associated with tumor progression via multiple effects including upregulation of angiogenic factors and proteases, increased invasion, and impaired immune functions. Tumors have been shown to adapt to pH changes and to grow at lower pHs than in normal tissues. It has been proposed that glycolysis is the main mechanism that lowers the pH of tumors, through generation of lactic acid. However, experiments with glycolysis-deficient cells indicate that production of lactic acid is not the only mechanism involved in the pH regulation of tumor cells. Carbonic anhydrases are a group of zinc-containing metalloenzymes that catalyze the reversible hydration of carbon dioxide to carbonic acid, providing a link between metabolism and pH regulation. The activities of the two isoformes, carbonic anhydrase IX and XII are reported to be strongly induced by hypoxia in a range of tumor cell lines. It has been proposed that these cancer-associated carbonic anhydrases might have a role in the regulation of pH balance during carcinogenesis and tumor progression. (Wykoff et al. 2000; Harris, 2002; Svastová et al. 2004)

Le *et al.* (2006) demonstrated in their study that tumor hypoxia exists in NSCLC and is associated with elevated expression of osteopontin (OPN) and CA IX. Carbonic anhydrase IX (CA IX) expression, which is strongly linked to HIF-1 activation, has been demonstrated in several tumor types. (Wykoff et al. 2000)

2.3.6 Hypoxia-inducible tumor-associated carbonic anhydrases

The thirteen active α-carbonic anhydrase (CA) isoenzymes participate in various biological processes, including ion transport and the maintenance of pH homeostasis.

They are physiologically important metalloenzymes that catalyze the reversible reaction; $CO_2 + H_2O \leftrightarrow H^+ + HCO_3^-$. High-activity CA isoforms have extremely fast turnover values hence they belong to the group of most efficient enzymes. The human α-CAs can be divided into three clusters, based on their phylogenetic relationships. The members of the evolutionary oldest cluster all contain an extracellular CA-domain of high- or medium-catalytic activity. This group contains transmembrane (CA IX, XII, XIV), membrane-associated via GPI anchor (CA IV, CA XV) and secreted (CA VI) isoenzymes. The second cluster consists of intracellular isoenzymes containing a single CA domain of either high (CA II, VA, VB, VII), medium (CA XIII) or low activity (CA I, CA III). The third cluster includes inactive cytoplasmic isoforms (CA XI, CA X, CAVIII). The α-CAs are expressed throughout the human body, some of them being ubiquitous or broadly distributed while others being confined to only a few tissues. (Pastorekova et al. 2006)

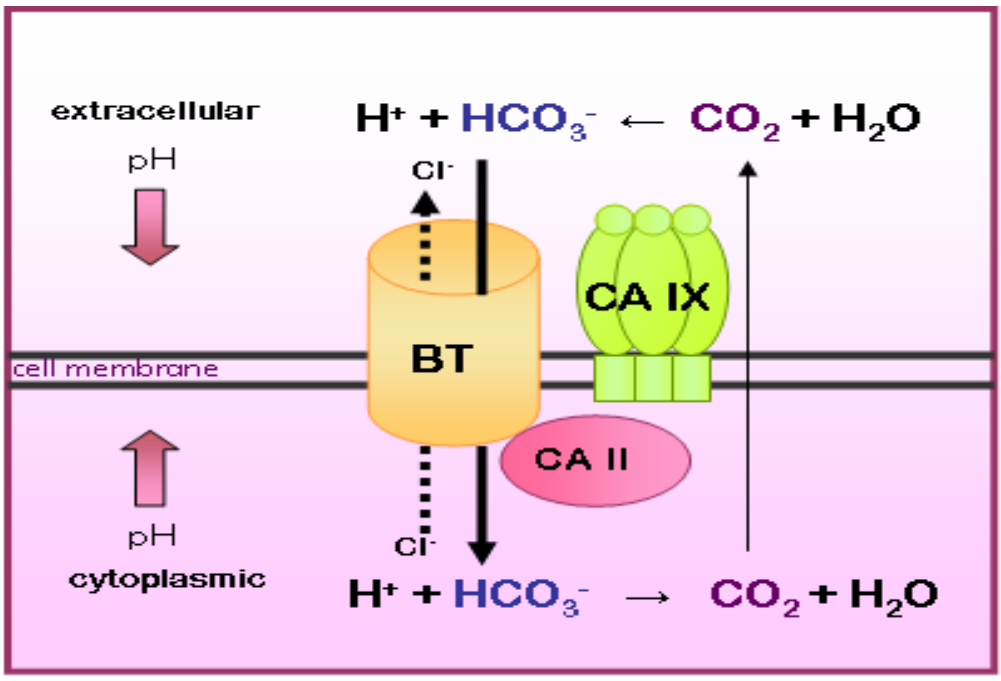

Figure 4. The proposed role of CA IX in the bicarbonate transport metabolon. CA IX acts as an extracellular component of the metabolon. It hydrates carbon dioxide and provides bicarbonate ions to bicarbonate transporter (BT) which could be for example an anion exchanger. BT transports bicarbonate ions to the cytoplasm in exchange for chloride anions. At the intracellular side, CA II converts bicarbonate to carbon dioxide, which diffuses out of the cell. Extracellular CA IX activity generates also protons and external pH lowers whereas intracellular pH neutralizes when intracellular activity of CA II consumes protons. Figure adapted from (Pastorekova et al. 2006).

Expression of different CA isoforms has been investigated in various types of malignancies. Two human isoenzymes, CA IX and CA XII, have been found to be overexpressed in cancer. (Pastorekova et al. 2006) These tumor-associated isozymes are proposed to acidify extracellular milieu surrounding the cancer cells and thus create a microenvironment conducive to tumor growth and spread. (Kivelä et al. 2005) The main mechanism of induction of CA IX and CA XII is hypoxia (Ivanov et al., 2001). Wykoff *et al.* showed in their study that CAs were up-regulated in pVHL-defective renal tumors, which indicates that they are expressed constitutively in pVHL-defective cells as a response to the HIF activation. (Wykoff et al. 2000)

CA IX protein is expressed only in few normal tissues but its expression is ectopically induced in many tumor types mainly due to its strong transcriptional activation by hypoxia through HIF-1. CA IX promoter has been proved to have a hypoxia response element (HRE) in its basal promoter (Wykoff et al., 2000). Although hypoxia also seems to increase *CA12* mRNA expression in some cell lines, a functional hypoxia responsive element has never been reported for the *CA12* gene. Consequently, it seems that CA XII is not as tightly regulated by HIF/pVHL pathway as CA IX. (Wykoff et al. 2000; Hynninen et al. 2006)

CA IX is a 459 amino acid glycoprotein that consists of a signal peptide, a proteoglycan-related sequence, a CA domain, a transmembrane segment and a short intracellular tail. CA IX expression was initially associated with cancer in HeLa cells by Zavada *et al.* in 1993. They observed that CA IX participated in oncogenesis and that its expression correlated with the tumorigenicity. CA XII was cloned and characterized by two groups almost simultaneously. (Ivanov et al. 1998; Tureci et al. 1998) The 354-amino acid CA XII polypeptide contains a signal sequence, a CA-domain, an additional short extracellular segment, a transmembrane segment and a C-terminal cytoplasmic tail. (Pastorekova et al. 2006)

Tumor growth involves complex interactions between cells and their microenvironment. Tumor microenvironment can be characterized by low acidic pH and altered hydrostatic and oxygen pressures. pH homeostasis is controlled in tumor cells by proton extrusion mechanisms. Tumor-associated CAs may have an important role in controlling the

levels of protons and bicarbonate ions in the tumor cells by sensing pH and tipping the proton balance across the cell membrane. The fact that CA IX and CA XII proteins are localized normally on differentiated cells specialized in acid/base homeostasis, for example the intercalated cells of the kidney and gastrointestinal gland cells, supports the proposed role for them in maintaining extracellular acidity in tumors. (Ivanov et al. 2001) The hypothetical role of CA IX in the pH regulation of tumors is represented in figure 4.

CA IX and XII are expressed in a broad range of different tumor types. For selected cancers, they may prove to be powerful diagnostic biomarkers. For example several studies have demonstrated that the expression of CA IX is an excellent diagnostic biomarker for renal cell carcinoma. (Ivanov et al. 2001; McKiernan et al. 1997)

2.3.7 Osteopontin

Osteopontin (OPN) is a secreted glycoprotein, which binds to integrin receptors, allowing OPN to mediate cell–cell and cell–matrix interactions. OPN has been found to be involved in multiple processes, including cell adhesion, invasion, and motility, both in tumor and normal cells. (Zhu et al. 2005) The protein has been shown to regulate cytokine production by macrophages, mediate neovascularization and inhibit apoptosis. It has also been shown that osteopontin maintains the homeostasis of free calcium. In addition of binding to integrin receptors, osteopontin also interacts with cells though CD44. (Weber, 2001; Rittling et al. 2004)

Osteopontin is an acidic glycoprotein with a molecular mass of approximately 44 kDa. It is rich in aspartate, glutamate and serine and contains about 30 monosaccharides, including 10 sialic acids. (Rangaswami et al. 2006; Weber, 2001) OPN was first identified as a major sialoprotein in bone (Oldberg et al. 1986). OPN is expressed in many different tissues, including dentin, kidney, vascular tissues, activated macrophages and lymphocytes. (Rangaswami et al. 2006)

Overexpression of osteopontin has been reported in a variety of cancers including breast (Tuck & Chambers, 2001) and prostate cancer (Thalmann et al. 1999), osteosarcoma

(Sulzbacher et al. 2002), glioblastoma (Said et al. 2007), SCC (Zhang et al. 2001) and melanoma (Zhou et al. 2005). Overexpression of osteopontin has also been demonstrated in NSCLC. (Donati et al. 2005; Hu et al. 2005) The mechanism behind the tumor growth regulation by OPN is still unclear. However, it has been suggested that OPN enhances growth of transformed cells, participates in pathways regulating migration, increases invasiveness, and acts together with several growth factors to induce malignant properties. (Rittling et al. 2004)
The regulation of OPN by hypoxia and re-oxygenation was first reported in 1994 by Hwang and collaborators (Hwang et al. 1994). To date, several studies have demonstrated that OPN is a hypoxia-inducible gene. For example Le *et al.* showed in 2003 that elevated plasma OPN levels correlated with tumor hypoxia and poor prognosis in head and neck cancer patients. (Le et al. 2003)

The mechanism of hypoxia induction of OPN is not fully known. The OPN promoter does not contain any of the known hypoxia response elements. Although hypoxia response elements seem to be required for transcriptional induction of many hypoxia-responsive genes, a number of different transcriptional binding sites have also been shown to be involved in hypoxic regulation of gene expression. In 2005 Zhu *et al.* identified, a *ras*-activated enhancer element in the OPN promoter that acts in both *ras* and hypoxic regulation of OPN expression. They also suggested a potential pathway for hypoxia induction of OPN that involves the Akt kinase. (Zhu et al. 2005)

As described above, osteopontin is present in tumors as well as some normal tissues. Additionally OPN is also found in body fluids, including blood and urine. Fedarko *et al.* measured OPN serum levels in patients with breast, colon, lung and prostate cancer and compared the results with control serum samples. They found elevated OPN levels in all tumor types except for colon cancer. (Fedarko et al. 2001) Plasma OPN has also been examined as a potential prognostic marker in head and neck cancers (Le et al. 2003). Consequently it has been proposed that OPN blood levels might have a potential as a prognostic or diagnostic marker. (Rittling et al. 2004)

2.5 Theoretical background

2.5.1 Circulating nucleic acids in plasma

It has been known for decades that blood plasma contains free circulating nucleic acids, RNA and DNA, and that the levels of circulating nucleic acids are higher in cancer patients than healthy controls. (Leon et al. 1977) Although the existence of extracellular RNA have been acknowledged for a long time, a relatively little is known about its biological significance. Circulating nucleic acids have been shown to share some biophysical properties, such as decreased strand stability, microsatellite alterations, and the presence of specific oncogene or tumor suppressor gene mutations, common to DNA of cancer cells. Therefore, it can be concluded that circulating nucleic acids could be originated from tumors. (Anker et al. 2001) Mutations in the *K-ras* proto-oncogene were the first mutations detected in the plasma of cancer patients. These gene mutations are frequently found in various types of cancers. (Bremnes et al. 2005)

Several studies have reported findings of different mRNA types in plasma or serum of cancer patients. There are high amounts of ribonucleases in plasma, particularly in the plasma of cancer patients. Thus one would predict that, as a labile molecule, all free RNA in the plasma would be degraded. However tumor-derived circulating RNA is protected from degradation by ribonucleases. (Bremnes et al. 2005) There have been a few suggestions of the possible mechanisms by which RNA is protected from ribonuclease activity. One proposed mechanism is that extracellular RNA and DNA are bound to each other in the plasma. This DNA-RNA hybrid would be resistant to nuclease activity. (Sisco, 2001) Other hypothesis is that the RNA is protected through binding to protein or lipoprotein complexes or that it is sequestered within lipid vesicles. Apoptotic vesicles that contained RNA were found in cultured tumor cell lines. The RNA of these vesicles was resistant to ribonucleases only when the vesicles remained intact. (El-Hefnawy et al. 2004)

Although it has been known for a long time that nucleic acids circulate freely in blood plasma both in disease and in health, the source of the extra-cellular nucleic acids remains enigmatic. Yet it is not known why cancer patients have larger quantities of

plasma nucleic acids, nor where this genetic material comes from. As with normal subjects, a proportion seems to originate from lymphocytes. However, a substantial proportion of plasma nucleic acids in cancer patients derive from tumor cells. The most common hypothesis is that the circulating nucleic acids derive from the lysis of circulating cancer cells or micrometastases shed by the tumor. This is evidently not the case since there are not enough circulating cells to justify the amount of DNA found in the plasma. It thus appears that tumor nucleic acids shed in the blood stream could be due either to leakage resulting from tumor necrosis or apoptosis or to a new mechanism of active release. It has also been hypothesized that the tumor actively releases DNA/RNA into the blood stream. Probably the presence of tumor-related nucleic acids in the plasma is the result, in variable proportions, of the different mechanisms which produce leakage or excretion of DNA and RNA. (Anker et al. 1999)

There is a need of novel tumor markers and for development of sensitive and specific non-invasive diagnostic tests for early detection and monitoring of recurrence. The analysis of circulating nucleic acids offers a possibility of finding tumor cell specific alterations in blood at a premalignant phase or an early stage of cancer. (Bremnes et al. 2005) Quantitative real-time polymerase chain reaction (qRT-PCR) is one possible method that can be used to detect tumor specific alterations in circulating RNA from plasma.

2.5.2 Quantitative real-time polymerase chain reaction (qRT-PCR)

Quantitative Real-time polymerase chain reaction (qRT-PCR) is a method that can be used to amplify and quantify nucleic acids. The procedure follows the general principle of polymerase chain reaction. When combined with reverse transcription polymerase chain reaction , qRT-PCR can be used to monitor gene expression by quantifying mRNA levels. It is the most sensitive technique for mRNA detection and quantification currently available. (Kubista et al. 2006)

qRT-PCR is based on detection of a fluorescent signal produced proportionally during amplification of a PCR product. The fluorescence will increase as the amount of the PCR product increases and it is quantified after each completed PCR cycle. The cycle at

which the fluorescence exceeds detection threshold background fluorescence, a parameter known as the threshold cycle (C_T) or crossing point (C_p), correlates to the number of target cDNA molecules present in the sample. During the first cycles the signal is weak and cannot be distinguished from the background. As the amount of product accumulates, a signal develops and increases exponentially. Eventually the signal levels off and saturates. The signal saturation is due to the reaction running out of some critical component. The amplification curves are separated in the growth phase of the reaction. This reflects the difference in their initial amounts of template molecules. An example of amplification curve is presented in figure 5. (Nolan et al. 2006; Kubitsa et al. 2006)

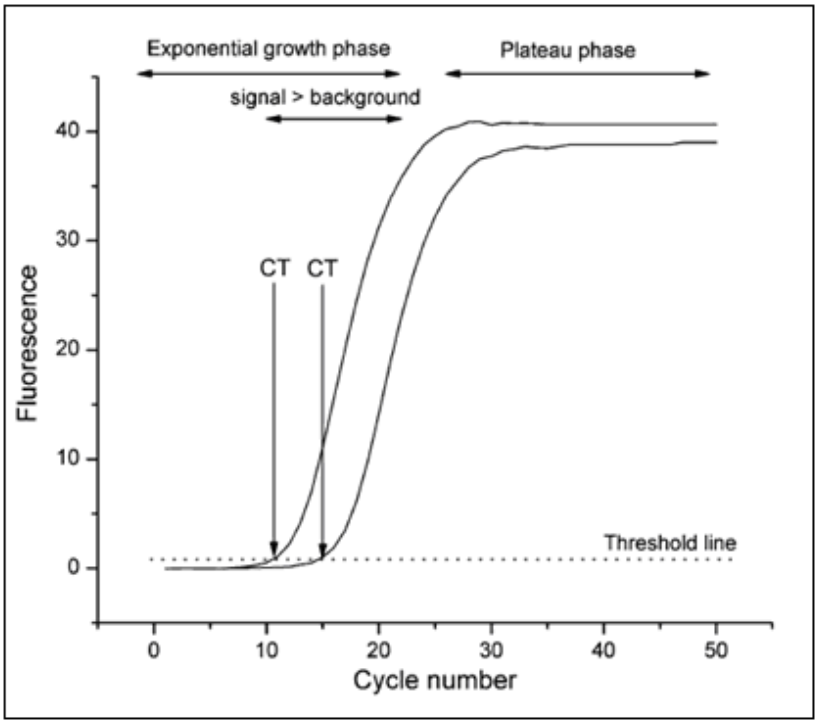

Figure 5. q-RT-PCR amplification curve. Figure from (Kubista et al. 2006).

There are two types of quantification methods; relative quantification and absolute quantification. In the absolute quantification, the target concentration is expressed as an absolute value i.e. a copy number or concentration. In the relative quantification the target concentration is expressed in relation to the concentration of a house-keeping gene and a standard curve is used to obtain the concentrations of the target and the house-keeping genes. (Giuletti et al. 2001)

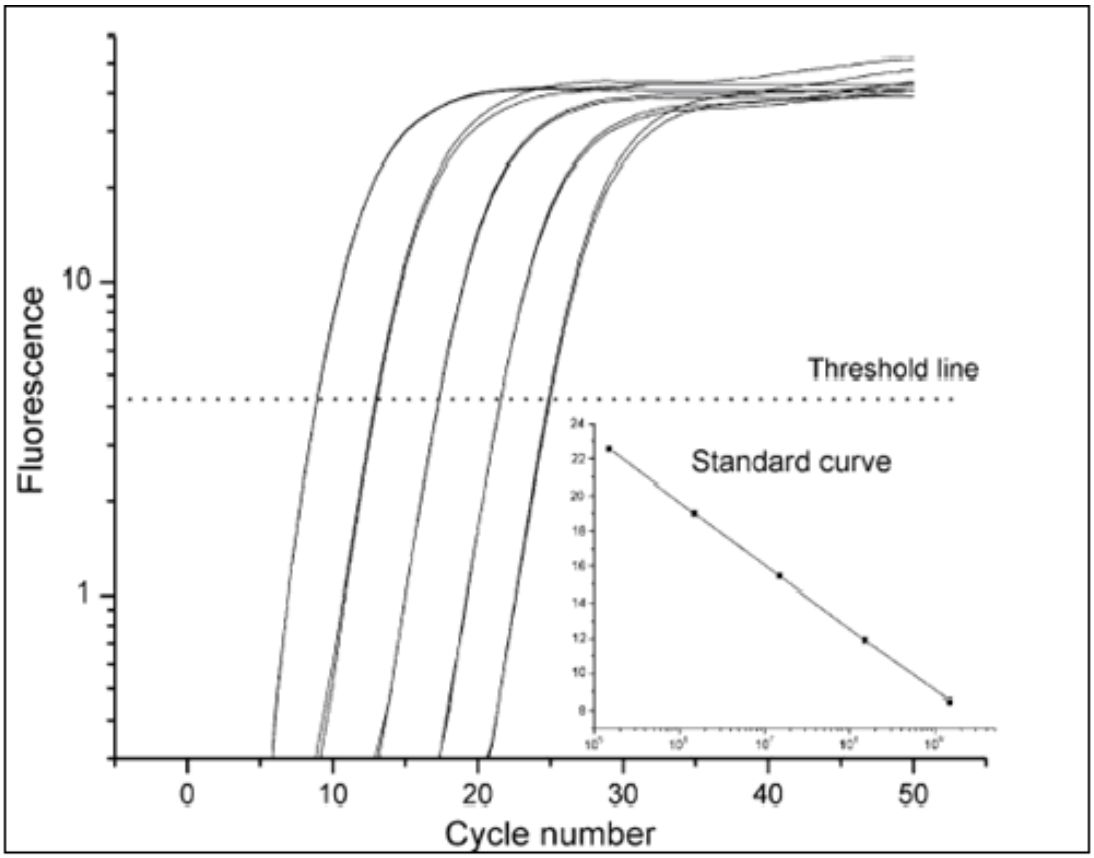

Figure 6. qRT-PCR standard curve. Amplification curves shown in logarithmic scale for five standard samples. The crossing points with threshold line are the C_t values. In the inset the C_t values are plotted vs. the logarithm of the initial number of template copies in the standard samples. Figure from (Kubista et al. 2006).

For the absolute quantification of the sample templates a standard curve is constructed from standards of known concentration. These standards can be a purified PCR product or a purified plasmid that contains the target sequence. The C_T values of the diluted standards are read out, and plotted versus the logarithm of the samples' concentrations, number of template copies or dilution factor (figure 6.). The standard curve produces a linear relationship between C_T and initial amounts of total RNA or cDNA, allowing the determination of the concentration of unknowns based on their C_T values.

Relative quantification is the most commonly used technique. It is a mathematical model that calculates changes in gene expression as a relative fold difference between an experimental and calibrator sample. While this method includes a correction for nonideal amplification efficiencies, the amplification kinetics of the target gene and reference gene assays must be approximately equal because different efficiencies will generate errors when using this method. Consequently, a validation assay must be performed where serial dilutions are assayed for the target and reference gene and the

results plotted with the log input concentration for each dilution on the x-axis, and the difference in C_T (target-reference) for each dilution on the y-axis. If the absolute value of the slope of the line is less than 0.1, the comparative C_T method may be used. The PCR product size should be kept small (less than 150 bp) and the reaction rigorously optimized. (Technical Notes NO. LC 10/2003, Roche; Wong & Medrano, 2005)

When studying gene expression, the quantity of the target gene transcript needs to be normalized against the quantity of a reference gene transcript in the same sample. Quantitative RT-PCR method requires correction for experimental variations due to differences in input RNA amount or in efficiencies of reverse transcription. The normalization is done by using housekeeping genes. An ideal housekeeping gene should be expressed at a constant level among different tissues of an organism, and should not be affected by experimental treatment itself. Because there is no gene that meets this criterion for every experimental condition, it is necessary to validate the expression stability of a control gene for the specific requirements of an experiment prior to its use for normalization. The various methods of normalization can be combined with different calculation methods, like the absolute standard curve method described previously. For example, when using relative quantification with external standards, a standard curve is used to obtain the concentration of the target and the reference gene. (Giuletti et al. 2001)

All the real-time PCR systems detect a fluorescent dye. The two most commonly used formats for detecting fluorescence are sequence-independent assays and sequence-specific assays. The sequence-independent assay relies on fluorophores that bind to all double-stranded DNA molecules regardless of sequence (for example SYBR Green I). Sequence-specific probe binding assays rely on fluorophores coupled to sequence-specific oligonucleotide hybridization probes, for example TaqMan-probes that only detect certain PCR products. (Technical Notes NO. 18/2004, Roche)

SYBR Green I binds to DNA double helix in a sequence-independent fashion. SYBR Green I barely fluoresces when it is free in solution, but its fluorescence emission is greatly enhanced when it binds to DNA, due to conformational changes in the dye. When SYBR Green I binds to dsDNA minor groove, its fluorescence emission increases over 100-fold. During the various stages of PCR, the intensity of the fluorescence signal

will vary, depending on the amount of dsDNA that is present. Thus, the increase in SYBR Green I signal correlates with the amount of product amplified during PCR. Since this assay detects both specific and non-specific PCR products, it must be carefully optimized and the product must be identified after the PCR run.

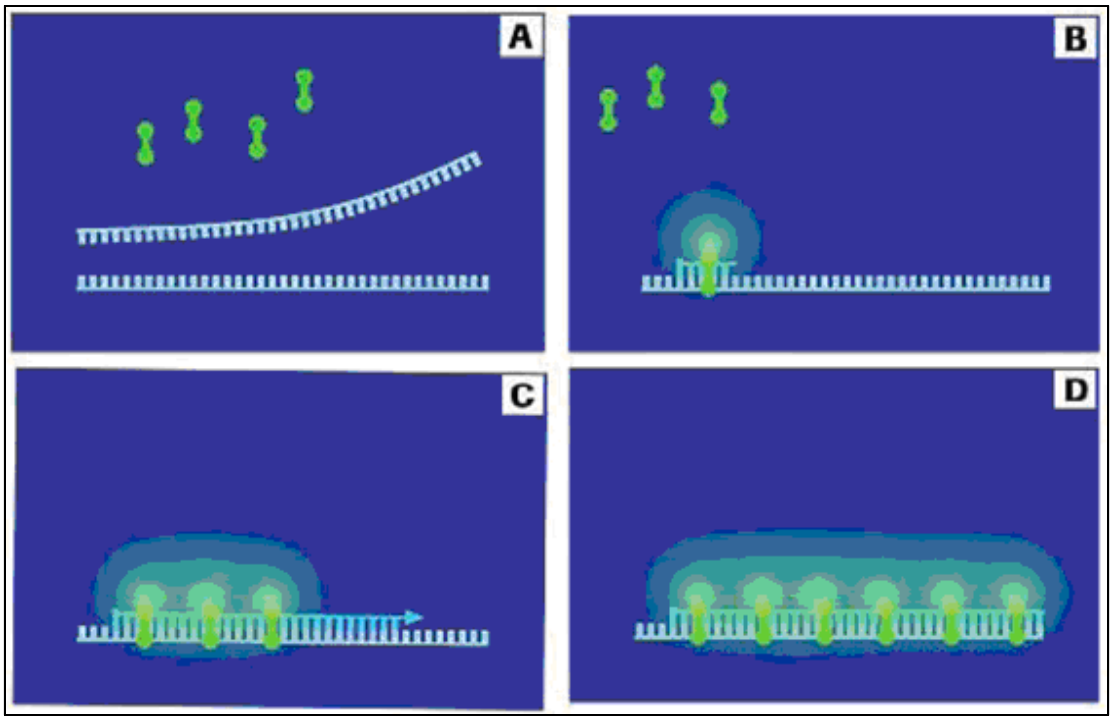

Figure 7. PCR reaction in the presence of SYBR Green I. Figure from (Technical Notes NO. 18/2004, Roche).

The PCR reaction with SYBR Green I is presented in figure 7. After denaturation, all DNA becomes single-stranded (Figure 7A). At this stage of the reaction, SYBR Green I dye will not bind and the fluorescence intensity is low. During annealing, the PCR primers hybridize to the target sequence creating small regions of double stranded DNA that SYBR Green I dye can bind, thereby leading to increased fluorescence (Figure 7B). In the elongation phase of PCR, PCR primers are extended and more SYBR Green I dye can bind (Figure 7C). At the end of the elongation phase, the entire DNA is double-stranded and a maximum amount of dye is bound (Figure 7D).

Since SYBR Green I binds to any double stranded DNA, it cannot discriminate between different double stranded DNA species. This is why the specific product, nonspecific products and primer-dimers are detected equally well. However, a melting curve analysis is an appropriate tool to discriminate between product and primer-dimer and

should always be included in the SYBR Green I program. (Technical Notes NO. 18/2004, Roche)

Sequence-specific assays use probes labeled with fluorophores. These assays are highly specific because fluorescence increases only if the specific target is present in the reaction. Due to this sequence specificity, non-specific by-products, such as primer-dimers or will not be detected and the product identification by melting curve analysis is usually not required.

Single-labelled probes are a special type of simplified hybridization probe that can detect mutations and single nucleotide polymorphisms (SNPs). The so-called simple probe format requires only one hybridization probe, labelled with only one fluorophore, to achieve sequence specificity. Typically such a probe is designed to specifically hybridize to a target sequence that contains the SNP of interest. Once hybridized to its target sequence, the SimpleProbe probe emits more fluorescence than it does when it is not hybridized. As a result, changes in fluorescence are based solely on the hybridization status of the probe. (Technical Notes NO. 18/2004, Roche)

3 Aims of the research

The aim of this research was to study mRNA expression levels of *HIF-1α* and three hypoxia-inducible genes, *CA9, CA12,* and *OPN,* in NSCLC patients' plasma and in healthy controls. mRNA expression was investigated by qRT-PCR, and the normalization was done using two house-keeping genes; beta-2-microglobulin and ubiquitin C. The results were analysed statistically. The aim was also to evaluate whether the studied genes would have potential as clinical tumor markers.

4 Methods

4.1 Patients and controls

The study population consisted of 95 cases of stage I-IIIA,B NSCLC patients (table 2.). The staging system describes the extent or severity of an individual's cancer. Stage 0 is carcinoma *in situ* which means that the cancer is in early phase and present only in the layer of cells in which it began. In stages I-III the higher numbers indicate more extensive disease and greater tumor size, and/or spread of the cancer to nearby lymph nodes or organs adjacent to the primary tumor. In stage IV the cancer has spread to another organ. (NCI, 2008)

Of all the cases 76 were males and 19 females. The mean age of patients was 69 years (range, 42-84 years). There were 36 squamous cell carcinoma, 17 adenocarcinoma, 30 large cell carcinoma, 2 other carcinomas and 10 without a definition of histology. The median follow-up of the NSCLC patients was 3.3 year (95% CI: 2.7 - 3.8 yr). The plasma samples of NSCLC patients were obtained from Dr. Philippe Lambin and Drs. Cary Dehing-Oberije (MAASTRO clinic, Maastricht, the Netherlands).

The controls consisting of 24 blood samples were collected from healthy volunteers. Peripheral blood sample was taken to a 4 mL sterile tube containing EDTA. After blood collection, the samples were centrifuged at 1500 x g at 4˚C for 15 min to separate the plasma and blood cells. The plasma samples were aliquoted and stored at -70˚C until analysis.

The World Health Organisation-performance scale (WHO-PS) and Charlson comorbidity index (CCI) are also presented in table 2. The WHO-PS describes the general wellbeing of the patients. It has categories from 0 to 4, in which 0 means that the patient is fully active and more or less as before the illness and 4 means that the patient is in severe condition. (WHO, 2008) The Charlson index is a validated scoring system of comorbidity that has been used for predicting patient mortality. (Hall et al., 2004)

Table 2. Patient characteristics

	all patients (n=95)
gender	
male	76 (80.0%)
female	19 (20.0%)
age	42-84 years (mean, 69 years)
WHO-PS	
0	28 (30.4%)
1	54 (58.7%)
>=2	10 (10.9%)
CCI	
0	27 (30.3%)
1	37 (41.6%)
2	16 (18.0%)
>=3	9 (10.0%)
histology	
SCC	36 (37.9%)
adenocarcinoma	17 (17.9%)
large cell carcinoma	30 (31.6%)
other	2 (2.1%)
no histology	10 (10.5%)
clinical stage	
I	18 (18.9%)
II	8 (8.4%)
IIIA	20 (21.1%)
IIIB	49 (51.6%)
gross tumor volume	1-674 ml (mean, 107 ml)
chemotherapy	
no	29 (31.2%)
yes	64 (68.8%)
OTT (days)	16 - 60 (mean, 34)

Abbreviations: WHO-PS = world health organisation - performance scale; CCI = Charlson comorbidity index; SCC = squamous cell carcinoma, OTT = overall treatment time

4.2 RNA extraction and DNase treatment

Total RNA was isolated from plasma samples using QIAamp® Viral RNA Mini kit (Qiagen, Hilden, Germany). The Spin protocol for purification of RNA from 140 µl of

plasma was performed according to the manufacturer's instructions. Prior to the RNA extraction, the samples were lysed under the highly denaturing conditions provided by buffer AVL to incativate RNases. The extracted RNA was eluted into 60 µl of AVE buffer. Eluted RNA was collected in standard 1.5 mL RNase-free microcentrifuge tubes.

RNA samples were treated with DNA-free™ Kit (Ambion, Austin, USA) DNase treatment was done to remove contaminating DNA, DNase and divalent cations from the samples. DNase treatment was done according to the protocol recommended by the manufacturer. The RNA samples were stored at -70˚C until analysis.

4.3 cDNA synthesis

Reverse transcription of the total RNA to cDNA was performed using the First Strand cDNA synthesis kit (Fermentas, Burlington, Canada). 1 µl of random hexamer primer (0,2 µg/µl) were mixed with 10 µl of total RNA. The final volume of this mixture was 11 µl. The samples were incubated for 5 min at 70 ºC and after that the tubes were chilled on ice. 4 µl of 5x reaction buffer, 1 µl of RiboLock™ Ribonuclease inhibitor (20u/µl) and 2 µl of 10 mM dNTP mix were added to the reaction mixture (all the reagents were from Fermentas). The samples were incubated for 5 min at room temperature. After incubation 2 µl of M-MuLV reverse transcriptase (20u/µl) was added. After adding the enzyme, the final volume of the mixture was 20 µl. The mixture was incubated at 25˚C for 10 minutes and finally at 37˚C for 60 minutes. The reaction was stopped by heating the tubes at 70˚C for 10 minutes.

4.4 qRT-PCR

HIF-1α, OPN, CA9, and *CA12* mRNA levels were measured from plasma samples by quantitative real-time PCR using the Lightcycler detection system (Roche, Rotkreuz, Switzerland). Two house-keeping genes, ubiquitin C (*UBC*) and beta-2-microglobulin (*B2M*) were used as reference genes to normalize the cDNA samples. *UBC* primers were obtained from RTprimerDB database with identification number 8. The other five RT-PCR primers were designed based on the complete cDNA sequences found in

GenBank. Accession numbers were NM_001530 for *HIF-1α*, NM_001040058 for *OPN,* NM_001216 for *CA9* and NM_001218 for *CA12*. The primers were designed so that, two primers from each primer set were located in different exons. This was done in order to avoid co-amplification of genomic DNA. The primer sequences used in this study and their annealing temperatures are shown in Table 1. The primers were produced by Oligomer (Helsinki, Finland).

Table 3. Primer sequences for quantitative real-time PCR used in the study.

gene		Sequence (5' - 3')	Length (bp)[a]	Accesion No.[b]	T_a (^oC)[c]
CA9	FW	GGAAGGCTCAGAGACTCA	160	NM_001216	53
	RW	CTTAGCACTCAGCATCAC			
CA12	FW	CTGCCAGCAACAAGTCAG	179	NM_001218	53
	RW	ATATTCAGCGGTCCTCTC			
HIF-1α	FW	TCACCTGAGCCTAATAGTCC	161	NM_001530	52
	RW	GCTAACATCTCCAAGTCTAA			
OPN	FW	GGCTGATTCTGGAAGTTCTG	98	NM_001040058	57
	RW	AGATTCTGCTTCTGAGATGG			
UBC[d]	FW	ATTTGGGTCGCGGTTCTTG	133	NM_021009	57
	RW	TGCCTTGACATTCTCGATGGT			
B2M	FW	GTATGCCTGCCGTGTGAA	84	NM_004048	52
	RW	CTCCATGATGCTGCTTAC			

Note. FW, forward primer; RW reverse primer; [a] Amplicon lenght in base pairs
[b] Genbank accession number of cDNA and corresponding gene,
available at http://www.ncbi.nim.nih.gov/. [c] T_a: annealing temperature;
[d] obtained from RTprimerDB database:http://medgen.ugent.be/rtprimerdb/index.php

The quantitative real-time polymerase chain reaction was performed in a total reaction volume of 20 µl containing 1.0 µl of first strand cDNA template, 0.5 µM of each primer and 1x of QuantiTect SYBR Green PCR Master Mix (Qiagen, Hilden, Germany). The PCR reaction was carried out as follows: firstly HotStartTaq DNA polymerase was activated by heating 15 min at 95^{o}C, temperature transition rate being 20^{o}C/s. Then the amplification was performed in a 3-step cycling procedure: denaturation at 95^{o}C, 15 s, temperature transition rate 20^{o}C/s; annealing temperature depending on the T_m for each primer pair, 20 s, temperature transition rate 20^{o}C/s; and elongation at 72^{o}C, 15 s, ramp rate 20^{o}C/s. The cycle number depends on the amount of template DNA. For *B2M*, *UBC*, *CA9*, and *OPN* the cycle number was 45 and for *CA12* and *HIF-1α* the cycle

number was 50. The final step was cooling step. Melting curve analysis was done every time after the run to check the purity of PCR products. Melting curve analysis permits the differentiation of specific product from non-specific products, such as primer dimers.

To quantify the RNA levels of the samples, a standard curve was established for each gene using 5-fold serial dilutions of known concentrations of purified PCR products generated from the same primer sets. By including a serial dilution of such a standard in each PCR run, with known amounts of input copynumber, the target gene can be quantified in the unknown samples. To construct the cDNA standards, PCR was performed to a cDNA sample from a tissue or a cell-line with known expression of the target gene. The PCR-reaction for creating the standards to each gene was performed by using the qRT-PCR primers. The amplicons of the PCR reaction were analyzed using a 1.2% agarose gel containing 0.1 µg/ml ethidium bromide (Sigma-Aldrich, Steinheim, Germany) with 100 bp DNA standard (New England Biolabs, Beverly, MA) and purified from the gel using CFX PCR DNA and Gel Band Purification Kit (GE Healthcare, Buckinghamshire, UK). Finally the cDNA concentrations were measured by optical density spectrophotometry at 260 and 280 nm. The copy number of standard DNA molecules was calculated by using the following equation (Equation 1) from QuantiTect SYBR Green PCR Handbook (11/2005).

(1) $$\frac{x\ \text{g/µl DNA}}{[\text{primer products in bp} \times 660\ ]} \times 6{,}022 \times 10^{23} = \text{Y molecules/µl}$$

Each cDNA sample was tested in duplicates and the obtained crossing point (Cp) value permitted the determination of the levels of starting message using a specific standard curve. The geometric mean of the two internal control genes was used as a normalization factor for gene expression levels. The relative mRNA expression was indicated as the copy number of target gene divided by the corresponding normalization factor.

4.4 Statistical analysis

Part of the statistical analysis was done by Drs. Cary Dehing-Oberije (MAASTRO clinic, Maastricht, the Netherlands). The analysis done by Drs. Cary Dehing-Oberije, were Wilcoxon Mann-Whitney test, correlation analysis and survival analysis. The non-parametric Wilcoxon Mann-Whitney test was used to analyse the statistically significant difference between RNA levels of healthy controls and NSCLC patients. The univariate Cox regression analysis, using the RNA levels as a continuous variable, was used in survival analysis. In addition, a multivariate analysis was performed using gross tumor volume, number of positive lymph node stations, gender and World Health Organization (WHO) performance status as a baseline model including the RNA variables one by one to assess their added value. Kaplan Meier Curves were used to assess the prognostic value of the dichotomized variables. The logrank test was applied if the Kaplan Meier curves did not cross.

Sensitivity and specificity were calculated by SPSS 13.0. The sensitivity and specificity of the investigated genes was examined by ROC curve analysis to evaluate their potential as tumor markers for diagnosis of lung cancer. Sensitivity was evaluated as the mean of confidence intervals of the area under the curve.

5 Results

5.1 qRT-PCR

The cDNA samples of NSCLC patients and healthy controls were tested in duplicates and the obtained crossing point (Cp) value permitted the determination of the levels of starting material using a specific standard curve. The mRNA levels were assessed in 24 plasma samples of healthy controls and 95 plasma samples of NSCLC patients. Detectable results were obtained for four different genes: two housekeeping genes, *UBC* and *B2M*, and to *OPN* and *HIF-1α*. CA IX and CA XII showed practically zero expression to all investigated samples. The mean C_P values of the all samples of NSCLC patients and controls for *UBC* and *B2M*, and to *OPN* and *HIF-1α* are represented in tables 4-7. Geometric mean values of the two house-keeping genes are presented in table 8. The relative mRNA expressions, indicated as the copy number of target gene divided by the geometric mean of the house-keeping genes are presented for *HIF-1α* and *OPN* in tables 9 and 10.

Table 4. The qRT-PCR results of *B2M* .

NSCLC patients								healthy controls	
sample	mean	sample	mean	sample	mean	sample	mean	sample	mean
1	10,0	25	76,6	49	16,8	73	88,1	1	14,0
2	44,8	26	7,4	50	91,0	74	46,1	2	12,8
3	8,6	27	24,2	51	14,3	75	8,8	3	27,9
4	21,2	28	17,1	52	111,6	76	67,9	4	1,0
5	13,0	29	3,3	53	7,4	77	33,4	5	22,3
6	93,2	30	8,4	54	86,5	78	25,2	6	18,9
7	10,8	31	7,7	55	593,9	79	81,6	7	91,6
8	1,3	32	4,5	56	1,1	80	218,7	8	1,6
9	11,4	33	30,4	57	2,1	81	205,1	9	5,1
10	2,3	34	92,9	58	218,3	82	195,8	10	5,6
11	36,3	35	82,2	59	592,8	83	63,9	11	75,4
12	1,5	36	148,2	60	7,8	84	57,7	12	13,6
13	0,2	37	141,4	61	46,1	85	123,8	13	19,7
14	1,4	38	133,4	62	133,4	86	243,8	14	34,7
15	0,3	39	199,0	63	577,7	87	117,6	15	108,0
16	11,0	40	79,5	64	13,7	88	9,5	16	9,0
17	53,5	41	31,2	65	5,1	89	114,5	17	15,1
18	112,1	42	51,7	66	149,7	90	309,6	18	2,3
19	15,9	43	3,8	67	89,3	91	6,5	19	6,2
20	225,0	44	51,9	68	173,4	92	651,8	20	1,2
21	145,1	45	2,1	69	37,0	93	32,6	21	1,3
22	7,3	46	11,9	70	6,0	94	234,3	22	145,0
23	9,2	47	15,1	71	1157,0	95	43,2	23	146,5
24	307,4	48	4,0	72	292,8			24	329,5

Table 5. The qRT-PCR results of *UBC*.

NSCLC patients								healthy controls	
sample	mean	sample	mean	sample	mean	sample	mean	sample	mean
1	1,6	25	38,7	49	43,3	73	25,5	1	13,90
2	4,5	26	5,3	50	428,6	74	12,6	2	1,30
3	23,0	27	35,0	51	0,0	75	5,7	3	2,00
4	1,2	28	0,0	52	126,2	76	12,7	4	29,10
5	6,4	29	10,2	53	18,6	77	13,7	5	10,40
6	6,4	30	22,8	54	13,8	78	9,2	6	8,70
7	46,1	31	11,0	55	457,8	79	15,9	7	0,00
8	24,6	32	6,7	56	36,2	80	44,8	8	4,20
9	8,5	33	30,0	57	0,0	81	42,7	9	0,00
10	0,0	34	44,5	58	0,0	82	26,4	10	0,80
11	16,7	35	35,0	59	512,7	83	8,8	11	10,10
12	12,7	36	33,6	60	0,0	84	11,6	12	3,30
13	0,0	37	70,1	61	73,8	85	21,9	13	6,30
14	0,6	38	321,5	62	107,5	86	81,1	14	6,40
15	13,8	39	83,7	63	327,0	87	37,8	15	50,30
16	5,2	40	65,0	64	29,9	88	6,4	16	10,40
17	27,4	41	8,8	65	42,2	89	102,2	17	50,60
18	38,2	42	35,8	66	64,0	90	105,0	18	0,00
19	63,0	43	0,0	67	43,2	91	88,0	19	0,00
20	43,8	44	24,3	68	30,0	92	123,3	20	0,00
21	54,0	45	9,7	69	12,3	93	9,9	21	0,00
22	13,7	46	12,6	70	30,5	94	102,3	22	18,40
23	11,8	47	100,7	71	374,9	95	196,3	23	15,00
24	121,0	48	0,6	72	284,6			24	283,90

Table 6. The qRT-PCR results of *OPN*.

NSCLC patients								healthy controls	
sample	mean	sample	mean	sample	mean	sample	mean	sample	mean
1	0,0	25	0,0	49	3,2	73	463,2	1	0,0
2	0,0	26	0,0	50	0,0	74	364,6	2	0,0
3	2,0	27	7,1	51	0,0	75	248,1	3	0,1
4	3,7	28	0,0	52	1,9	76	18,2	4	0,0
5	0,0	29	0,0	53	0,0	77	66,7	5	0,4
6	0,0	30	0,0	54	0,0	78	88,5	6	0,0
7	0,0	31	0,0	55	0,2	79	106,3	7	7,2
8	0,0	32	2,8	56	0,0	80	21,6	8	0,0
9	0,0	33	2,0	57	1037,8	81	63,1	9	0,0
10	0,0	34	3,8	58	1585,5	82	39,3	10	2,6
11	0,0	35	0,0	59	2975,0	83	19,3	11	0,0
12	0,8	36	0,0	60	39,2	84	62,2	12	0,0
13	0,0	37	5,5	61	837,5	85	10,6	13	3,8
14	0,0	38	0,0	62	0,0	86	82,6	14	4,0
15	0,0	39	0,0	63	1048,6	87	42,2	15	0,0
16	0,0	40	5,6	64	2839,5	88	24,9	16	0,0
17	0,0	41	0,1	65	3394,0	89	149,3	17	0,0
18	0,0	42	0,3	66	2533,0	90	27,4	18	0,0
19	0,0	43	2,4	67	1461,0	91	51,4	19	0,0
20	3,1	44	4,7	68	1560,5	92	6,7	20	4,9
21	3,7	45	1,2	69	144,4	93	7,4	21	0,0
22	0,0	46	5,5	70	131,2	94	0,1	22	0,0
23	0,0	47	2,1	71	670,9	95	9,3	23	4,1
24	0,0	48	4,1	72	939,3			24	7,5

Table 7. The qRT-PCR results of *HIF-1α*.

NSCLC patients								healthy controls	
sample	mean	sample	mean	sample	mean	sample	mean	sample	mean
1	1,2	25	9,7	49	0,3	73	0,7	1	0,8
2	0,5	26	3,7	50	0,7	74	0,7	2	0,6
3	0,5	27	9,1	51	0,1	75	0,0	3	0,6
4	0,3	28	3,8	52	3,5	76	3,5	4	1,1
5	0,6	29	2,0	53	4,2	77	2,1	5	0,9
6	0,3	30	1,9	54	12,0	78	11,1	6	0,8
7	0,8	31	1,4	55	1,3	79	0,0	7	3,2
8	1,5	32	2,5	56	25,8	80	21,0	8	6,1
9	1,2	33	1,8	57	4,3	81	81,9	9	7,6
10	2,7	34	3,7	58	11,6	82	2,1	10	6,6
11	1,1	35	3,2	59	11,6	83	1,5	11	7,2
12	4,4	36	3,5	60	5,9	84	3,6	12	8,8
13	1,6	37	7,1	61	20,0	85	62,0	13	10,2
14	3,1	38	4,4	62	6,3	86	11,9	14	5,7
15	3,9	39	2,8	63	17,0	87	5,0	15	4,1
16	3,1	40	5,5	64	3,6	88	36,4	16	3,4
17	2,1	41	0,6	65	4,7	89	3,7	17	3,4
18	3,1	42	19,2	66	6,0	90	6,4	18	10,0
19	0,9	43	274,4	67	4,9	91	5,0	19	2,1
20	4,2	44	9,0	68	7,6	92	6,6	20	6,1
21	10,7	45	0,5	69	0,7	93	1,4	21	7,4
22	7,6	46	27,9	70	3,4	94	3,8	22	10,0
23	10,3	47	31,6	71	17,4	95	5,7	23	6,6
24	177,3	48	379,6	72	7,1			24	59,6

Table 8. The qRT-PCR results of *B2M+UBC* (geometric mean).

NSCLC patients								healthy controls	
sample	mean	sample	mean	sample	mean	sample	mean	sample	mean
1	4,0	25	54,4	49	27,0	73	47,4	1	13,9
2	14,2	26	6,3	50	197,5	74	24,1	2	4,1
3	14,0	27	29,1	51	-	75	7,1	3	7,4
4	5,0	28	-	52	118,6	76	29,4	4	5,3
5	9,1	29	5,8	53	11,7	77	21,4	5	15,2
6	24,5	30	13,9	54	34,6	78	15,3	6	12,8
7	22,3	31	9,2	55	521,4	79	36,0	7	-
8	5,7	32	5,5	56	6,2	80	98,9	8	2,6
9	9,8	33	30,2	57	-	81	93,6	9	-
10	0,0	34	64,3	58	-	82	71,9	10	2,1
11	24,6	35	53,7	59	551,3	83	23,8	11	27,6
12	4,4	36	70,6	60	0,0	84	25,8	12	6,7
13	-	37	99,5	61	58,3	85	52,0	13	11,2
14	0,9	38	207,1	62	119,7	86	140,6	14	14,9
15	1,9	39	129,1	63	434,6	87	66,7	15	73,7
16	7,6	40	71,9	64	20,2	88	7,8	16	9,7
17	38,3	41	16,6	65	14,7	89	108,1	17	27,6
18	65,5	42	43,0	66	97,9	90	180,3	18	-
19	31,7	43	-	67	62,2	91	24,0	19	-
20	99,3	44	35,5	68	72,1	92	283,5	20	-
21	88,5	45	4,6	69	21,3	93	17,9	21	0,2
22	10,0	46	12,3	70	13,6	94	154,8	22	51,6
23	10,4	47	39,0	71	658,6	95	92,0	23	46,9
24	192,8	48	1,5	72	288,7			24	305,8

Table 9. The qRT-PCR results of *OPN / B2M+UBC*.

NSCLC patients								healthy controls	
sample	mean	sample	mean	sample	mean	sample	mean	sample	mean
1	0,0	25	0,0	49	0,1	73	9,8	1	0,0
2	0,0	26	0,0	50	0,0	74	15,1	2	0,0
3	0,1	27	0,2	51	0,0	75	35,0	3	0,0
4	0,7	28	0,0	52	0,0	76	0,6	4	0,0
5	0,0	29	0,0	53	0,0	77	3,1	5	0,0
6	0,0	30	0,0	54	0,0	78	5,8	6	0,0
7	0,0	31	0,0	55	0,0	79	3,0	7	0,0
8	0,0	32	0,5	56	0,0	80	0,2	8	0,0
9	0,0	33	0,1	57	0,0	81	0,7	9	0,0
10	0,0	34	0,1	58	0,0	82	0,5	10	1,3
11	0,0	35	0,0	59	5,4	83	0,8	11	0,0
12	0,2	36	0,0	60	0,0	84	2,4	12	0,0
13	0,0	37	0,1	61	14,4	85	0,2	13	0,3
14	0,0	38	0,0	62	0,0	86	0,6	14	0,3
15	0,0	39	0,0	63	2,4	87	0,6	15	0,0
16	0,0	40	0,1	64	140,4	88	3,2	16	0,0
17	0,0	41	0,0	65	230,8	89	1,4	17	0,0
18	0,0	42	0,0	66	25,9	90	0,2	18	0,0
19	0,0	43	0,0	67	23,5	91	2,1	19	0,0
20	0,0	44	0,1	68	21,6	92	0,0	20	0,0
21	0,0	45	0,3	69	6,8	93	0,4	21	0,0
22	0,0	46	0,4	70	9,7	94	0,0	22	0,0
23	0,0	47	0,1	71	1,0	95	0,1	23	0,1
24	0,0	48	2,7	72	3,3			24	0,0

Table 10. The qRT-PCR results of *HIF-1*α / B2M+UBC.

NSCLC patients								healthy controls	
sample	mean	sample	mean	sample	mean	sample	mean	sample	mean
1	0,3	25	0,2	49	0,0	73	0,0	1	0,1
2	0,0	26	0,6	50	0,0	74	0,0	2	0,2
3	0,0	27	0,3	51	0,0	75	0,0	3	0,1
4	0,1	28	0,0	52	0,0	76	0,1	4	0,2
5	0,1	29	0,3	53	0,4	77	0,1	5	0,1
6	0,0	30	0,1	54	0,3	78	0,7	6	0,1
7	0,0	31	0,2	55	0,0	79	0,0	7	0,0
8	0,3	32	0,5	56	4,2	80	0,2	8	2,3
9	0,1	33	0,1	57	0,0	81	0,9	9	0,0
10	0,0	34	0,1	58	0,0	82	0,0	10	3,2
11	0,0	35	0,1	59	0,0	83	0,1	11	0,3
12	1,0	36	0,1	60	0,0	84	0,1	12	1,3
13	0,0	37	0,1	61	0,3	85	1,2	13	0,9
14	3,3	38	0,0	62	0,1	86	0,1	14	0,4
15	2,0	39	0,0	63	0,0	87	0,1	15	0,1
16	0,4	40	0,1	64	0,2	88	4,7	16	0,3
17	0,1	41	0,0	65	0,3	89	0,0	17	0,1
18	0,0	42	0,4	66	0,1	90	0,0	18	0,0
19	0,0	43	0,0	67	0,1	91	0,2	19	0,0
20	0,0	44	0,3	68	0,1	92	0,0	20	0,0
21	0,1	45	0,1	69	0,0	93	0,1	21	43,8
22	0,8	46	2,3	70	0,3	94	0,0	22	0,2
23	1,0	47	0,8	71	0,0	95	0,1	23	0,1
24	0,9	48	253,2	72	0,0			24	0,2

The expression of the *B2M*, *UBC*, *HIF-1α* and *OPN* were detected in plasma of both NSCLC patients and control subjects. The difference in mRNA levels between NSCLC patients and healthy controls was tested for the tumor-related genes as well as the housekeeping genes (Table 11). The P-values based on the non-parametric Wilcoxon Mann-Whitney test showed a statistically significant difference between healthy controls and NSCLC patients for *UBC* as well as *HIF-1α* and *OPN* corrected for the housekeeping genes.

Table 11. mRNA levels in blood plasma

	Healthy controls					NSCLC patients					
Gene	Mean	SD	Median	Range	N	Mean	SD	Median	Range	N	P*
UBC	21.9	57.6	6.4	0.0 – 283.9	24	60.1	101.5	25.5	0,0 – 512.7	95	0.001
B2M	46.2	75.1	14.5	1.0 – 329.5	24	102.9	172.1	43.2	0.2 – 1157.0	95	0.056
UBC+B2M					19						0.067
OPN	1.4	2.4	0	0.0 – 7.5	24	594.1	930.4	88.5	0.0 – 3394.0	39	<0.001
OPN/UBC					24					39	<0.001
OPN/B2M					24					39	<0.001
OPN/ B2M+UBC					24					39	<0.001
HIF-1α	7.2	11.6	5.9	0.6 – 59.6	24	15.9	51.1	3.7	0.0 – 379.6	95	0.716
HIF-1α/UBC					24					95	0.435
HIF-1α/B2M					24					95	0.052
HIF1α/ UBC+B2M					24					95	0.576

Abbrevations; SD = standard deviation.

* P-value based on the Wilcoxon Mann-Whitney test

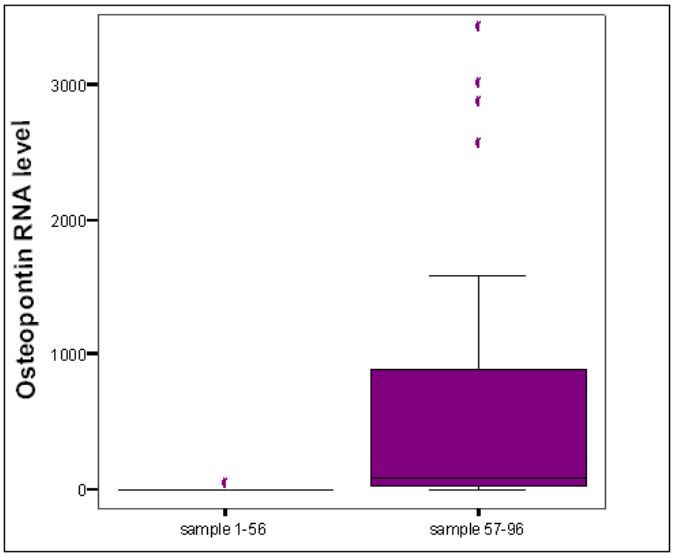

Figure 8. Osteopontin mRNA levels

The boxplot analysis of *OPN* mRNA levels is presented in figure 8. The samples 1-56 showed very low amounts of mRNA compared to samples 57-95 although all thesamples have been processed exactly in the same way. This was taken into account when analyzing the data and the statistical analysis for OPN is based on the last 39 samples. The explanation of the skewed result could be that the samples 1-56 could represent different patient categories compared to 57-95. For example they could belong to different categories ragarding to tumor histology.

5.2 Correlation analysis

Table 12. Spearman's correlations between mRNA levels of different genes and proteins measured in blood plasma

Genes		Interleukin-6	Interleukin-8	CEA	CYFRA 21-1	OPN
B2M	Correlation	0.08	0.07	-0.10	0.02	0.12
	Sig. (2-tailed)	0.462	0.475	0.328	0.849	0.256
	N	95	94	95	95	93
UBC	Correlation	-0.04	0.01	-0.16	-0.07	0.19
	Sig. (2-tailed)	0.696	0.941	0.122	0.509	0.068
	N	95	94	95	95	93
B2M + UBC	Correlation	0.01	0.03	-0.13	-0.07	0.15
	Sig. (2-tailed)	0.937	0.763	0.195	0.525	0.164
	N	95	94	95	95	93
HIF-1α	Correlation	-0.05	0.19	0.04	0.15	0.06
	Sig. (2-tailed)	0.640	0.073	0.714	0.142	0.567
	N	95	94	95	95	93
HIF-1α /UBC	Correlation	-0.03	0.09	0.11	0.05	-0.15
	Sig. (2-tailed)	0.777	0.424	0.293	0.635	0.156
	N	87	86	87	87	86
HIF-1α /B2M	Correlation	-0.12	0.09	0.08	0.06	-0.14
	Sig. (2-tailed)	0.253	0.382	0.447	0.555	0.186
	N	95	94	95	95	93
HIF-1α /both	Correlation	-0.09	0.06	0.13	0.05	-0.14
	Sig. (2-tailed)	0.393	0.593	0.221	0.649	0.200
	N	87	86	87	87	86
OPN	Correlation	0.05	-0.05	0.01	0.12	-0.01
	Sig. (2-tailed)	0.779	0.775	0.949	0.484	0.959
	N	39	38	39	39	37
OPN/B2M	Correlation	-0.03	-0.16	-0.01	0.07	-0.03
	Sig. (2-tailed)	0.870	0.325	0.932	0.679	0.838
	N	39	38	39	39	37
OPN/UBC	Correlation	-0.06	-0.10	0.07	0.04	-0.07
	Sig. (2-tailed)	0.715	0.570	0.677	0.798	0.702
	N	36	35	36	36	35
OPN/both	Correlation	-0.05	-0.10	0.04	0.06	-0.03
	Sig. (2-tailed)	0.764	0.558	0.803	0.731	0.848
	N	36	35	36	36	35

A correlation analysis was performed for the NSCLC patients. The correlation between the RNA levels and a number of biomarker, measured in blood plasma, as well as clinical characteristics was investigated. No correlation between blood biomarkers and RNA levels in blood was found to be statistically significant. The highest correlation of the clinical characteristics was found between osteopontin mRNA levels and SUVmax (maximum Standardized Uptake Value) measured on PET scan. Correlation analysis is represented in tables 12 and 13.

Table 13. Spearman's correlation between mRNA levels and clinical factors

		PLNS	N stage	TNM stage	SUVmax	GTV 1	GTV 2	GTV	Age	lung toxicity score
B2M	Correlation	-0.01	-0.02	0.07	-0.16	0.18	-0.18	0.08	0.07	-0.10
	Sig. (2-	0.956	0.834	0.518	0.526	0.091	0.098	0.47	0.52	0.346
	N	78	95	95	18	94	87	87	95	89
UBC	Correlation	0.04	-0.05	0.05	-0.25	0.01	-0.10	0.00	0.05	-0.04
	Sig. (2-	0.756	0.614	0.623	0.311	0.921	0.335	0.99	0.59	0.684
	N	78	95	95	18	94	87	87	95	89
UBC+B2M	Correlation	0.00	-0.03	0.09	-0.17	0.08	-0.15	0.02	0.04	-0.07
	Sig. (2-	0.984	0.808	0.390	0.499	0.449	0.171	0.83	0.71	0.536
	N	78	95	95	18	94	87	87	95	89
OPN	Correlation	-0.13	-0.21	-0.07	-.593(*)	0.02	-0.28	-0.03	-0.08	0.20
	Sig. (2-	0.476	0.208	0.665	0.033	0.892	0.082	0.85	0.63	0.234
	N	32	39	39	13	39	39	39	39	37
OPN/B2M	Correlation	-0.11	-0.18	-0.08	-0.43	-0.12	-0.21	-0.14	-0.07	.329(*)
	Sig. (2-	0.554	0.272	0.624	0.138	0.473	0.191	0.40	0.69	0.047
	N	32	39	39	13	39	39	39	39	37
OPN/UBC	Correlation	-0.08	0.04	0.11	-0.28	0.02	-0.14	0.02	-0.21	0.24
	Sig. (2-	0.664	0.798	0.534	0.354	0.893	0.423	0.92	0.21	0.159
	N	30	36	36	13	36	36	36	36	35
OPN/both	Correlation	-0.08	-0.04	0.06	-0.37	-0.02	-0.22	-0.04	-0.18	0.27
	Sig. (2-	0.682	0.826	0.746	0.209	0.919	0.192	0.82	0.29	0.115
	N	30	36	36	13	36	36	36	36	35
HIF-1α	Correlation	0.12	0.03	0.12	-0.15	0.11	0.07	0.18	0.13	-0.09
	Sig. (2-	0.309	0.784	0.234	0.548	0.300	0.550	0.09	0.22	0.393
	N	78	95	95	18	94	87	87	95	89
HIF-1α /B2M	Correlation	0.08	0.02	-0.01	0.04	-0.08	0.16	0.05	0.09	0.02
	Sig. (2-	0.504	0.871	0.919	0.874	0.459	0.138	0.64	0.39	0.839
	N	78	95	95	18	94	87	87	95	89
HIF-1α /UBC	Correlation	0.01	0.05	0.08	0.13	0.06	0.10	0.12	0.13	-0.07
	Sig. (2-	0.946	0.653	0.488	0.604	0.596	0.381	0.29	0.23	0.551
	N	72	87	87	18	86	79	79	87	82
HIF-1α /both	Correlation	0.06	0.01	0.03	0.05	-0.01	0.12	0.08	0.15	-0.02
	Sig. (2-	0.589	0.931	0.789	0.855	0.897	0.313	0.50	0.15	0.883
	N	72	87	87	18	86	79	79	87	82

Abbreviations: PLNS = number of positive lymf node stations; SUVmax = maximum standardized uptake value on PET-scan
GTV1 = gross tumor volume primary tumor; GTV2 = gross tumor volume nodes; GTV = total gross tumor volume

5.3 Survival analysis

The univariate Cox regression analysis did not show any significant relationship between survival and mRNA level. In addition, a multivariate analysis was performed using gross tumor volume, number of positive lympf node stations, gender and WHO performance status as a baseline model and including the mRNA variables one by one to assess their added value. These results, in terms of p-values, are shown in table 14.

Table 14. Results Cox Regression Analysis (p-values)

	Univariate	Multivariate*
UBC	0.901	0.581
B2M	0.419	0.327
UBC+B2M	0.868	0.440
OPN	0.941	0.805
OPN/UBC	0.66	0.704
OPN/B2M	0.227	0.583
OPN/both	0.994	0.350
HIF-1α	0.107	0.711
HIF-1α /UBC	0.277	0.391
HIF-1α /B2M	0.105	0.616
HIF-1α /both	0.267	0.390

*P-value corrected for tumor volume, number of positive lymph node stations, WHO performance status and gender

5.4 Roc curve analysis

To examine the sensitivity and specificity of potential tumor markers, a ROC curve analysis was performed. The sensitivity and specificity values were calculated as the mean of confidence intervals of area under the curves. Receiver-operating characteristic (ROC) analysis was done to the two house-keeping genes, to *OPN* and *HIF-1α* and to *HIF-1α* and *OPN* corrected for the housekeeping genes (Table 15). The ROC curve analysis of *UBC*, *B2M*, *HIF-1α* and *OPN* mRNA expression are presented in figures 9-11.

Table 15. ROC analysis.

	Cases					Asymptotic 95% Confidence Interval	
Variable	NSCLC	Controls	Area	Std. Error[a]	Asymptotic Sig.[b]	Lower Bound	Upper Bound
B2M	93	24	0,621	0,062	0,069	0,498	0,743
UBC	93	24	0,734	0,057	0	0,621	0,846
B2M+UBC	87	19	0,68	0,066	0,014	0,55	0,81
OPN	93	24	0,681	0,053	0,006	0,578	0,784
OPN/B2M	93	24	0,676	0,055	0,008	0,569	0,783
OPN/UBC	90	22	0,679	0,057	0,009	0,567	0,791
OPN/B2M+UBC	90	22	0,689	0,055	0,006	0,58	0,797
HIF*	93	24	0,529	0,063	0,666	0,406	0,652
HIF/B2M*	93	24	0,624	0,058	0,062	0,51	0,738
HIF/UBC*	86	19	0,691	0,067	0,009	0,559	0,823
HIF/B2M+UBC*	86	19	0,672	0,059	0,019	0,557	0,787

[a] Under the nonparametricassumption

[b] Null hypothesis: true area = 0.5

* Smaller test results indicates more positive test

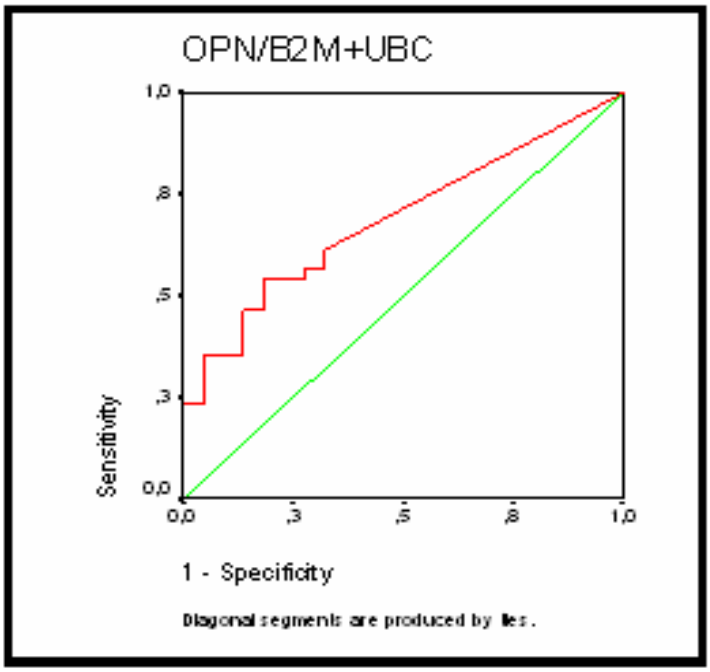

Figure 9. ROC analysis of *OPN* mRNA expression corrected for the B2M+UBC geometric mean.

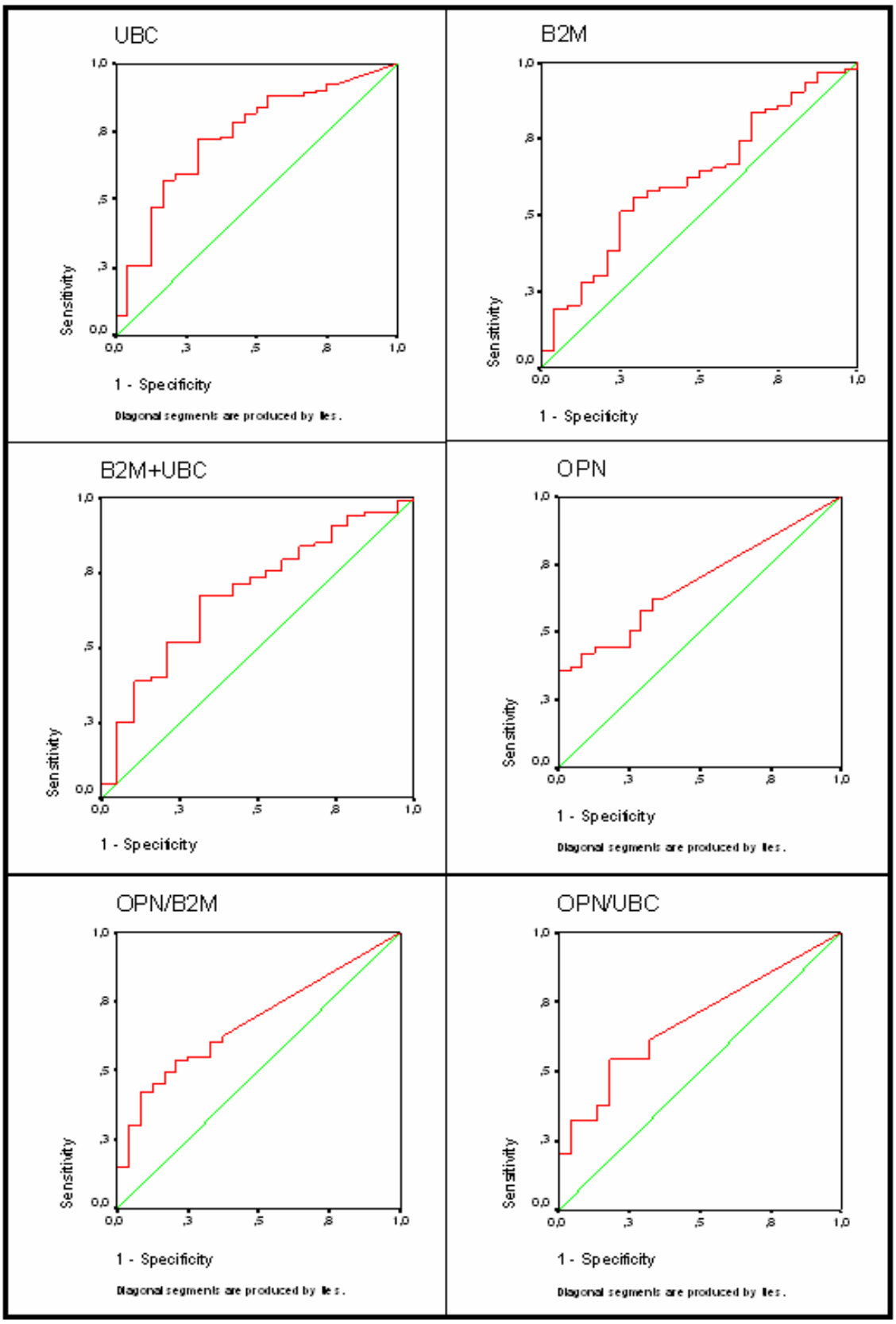

Figure 10. ROC analysis of the mRNA expressions of *B2M*, *UBC*, *B2M+UBC* (geometric mean), *OPN*, *OPN* corrected for the *B2M* and *OPN* corrected for the *UBC*.

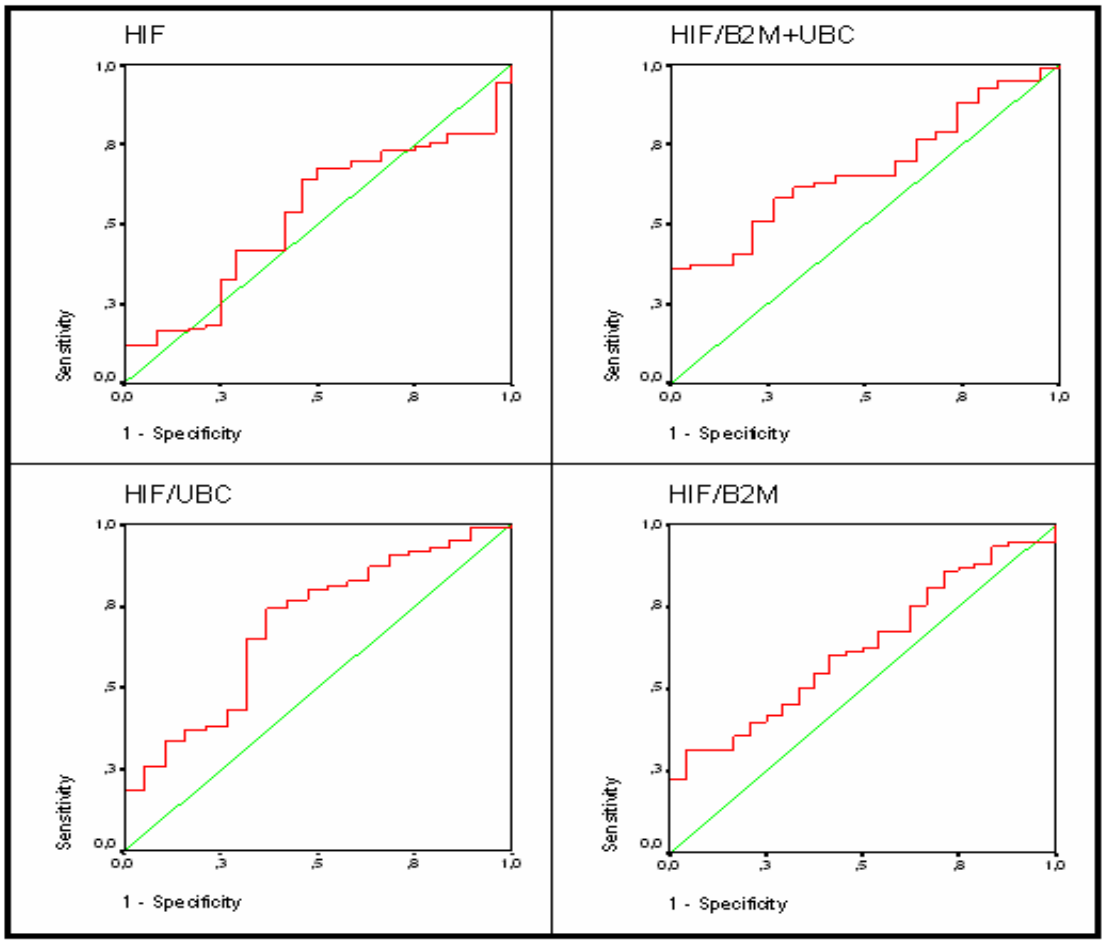

Figure 11. ROC analysis of the mRNA expressions of *HIF-1α*, *HIF-1α* corrected for the *B2M+UBC*, *HIF-1α* corrected for the *B2M* and *HIF- 1α* corrected for the *UBC*.

6 Discussion

Lung cancer is the most frequent cancer in the world, both in terms of incidence and mortality. (Donati et al. 2005) In recent years serum/plasma biomarkers have not been available as an effective clinical tool in screening or early diagnosis of lung cancer. The discovery of new potential biomarkers would have positive impact on the clinical outcome of lung cancer patients by helping to reflect the disease activity and predict/monitor response to therapy. (Bharti et al. 2007)

Several studies have provided the evidence that tumor-like nucleic acids are present in plasma of cancer patients and can be detected with sensitive techniques (Tong et al. 2006). Although small amounts of free nucleic acids circulate in both healthy and diseased human plasma, nucleic acid concentration is increased in the cancer patients' plasma. (Anker et al. 1999) The discovery of circulating nucleic acids has opened up new possibilities for non-invasive detection and monitoring of various cancers. The detection and quantification of circulating nucleic acids have shown to be promising for cancer diagnosis and prognosis. (Tong et al. 2006) It has also been demonstrated that the plasma nucleic acids levels are not only greater in cancer patients than in normal subjects but also correlate inversely with outcome and tend to fall with effective treatment. (Anker et al. 2006) Circulating tumor nucleic acids carrying several cancerous molecular changes have been reported in the plasma of patients with NSCLC. (Esteller et al. 1999; Sánchez-Céspedes et al. 1998)

Hypoxia is associated with malignant progression and poor outcome in human cancers. The effect of hypoxia on malignant progression is mediated by a series of hypoxia-induced proteomic and genomic changes activating angiogenesis, anaerobic metabolism, and other processes that enable tumor cells to survive or escape their oxygen deficient environment. (Simi et al. 2006) Hypoxia-inducible factors mediate the activation of a conserved transcriptional program that assists cells to adapt to hypoxia. (Wouters et al. 2005) HIF-1α is the regulatory subunit of HIF-1 that is stabilized and dimerized with HIF-1β under hypoxic conditions. HIF-1 α activity *in vivo* has been found to promote tumor growth and resistance to various chemotherapy agents.

Swinson *et al.* showed in 2004 that HIF-1α is commonly expressed in NSCLC. (Swinson et al. 2004)

CA IX and CA XII are transmembrane enzymes that catalyze the reversible hydration of carbon dioxide into carbonic acid (Pastorekova et al. 2004) *CA9* and *CA12* gene expression levels are strongly up-regulated via HIF-1. Several studies have reported that CA IX is overexpressed in NSCLC. (Simi et al. 2006; Kim et al. 2004)

Osteopontin is a hypoxia-inducible gene that is classified both as a matrix protein and a cytokine, which can be found in the ECM components and many body fluids (Hu et al. 2005). Osteopontin is reported to be one of the most overexpressed genes in a differential expression cDNA library derived from NSCLC (Bogenrieder & Herlyn, 2003). Hu *et al.* demonstrated in 2004 that osteopontin plays an important role in during development and progression of NSCLC (Hu et al. 2004).

In this study, the goal was to measure mRNA expression levels of *HIF-1α* and three hypoxia-inducible genes, *CA9, CA12* and *OPN,* in NSCLC patients' plasma using quantitative real-time polymerase chain reaction and clarify their clinical significance as potential plasma biomarkers for lung cancer. mRNA levels were assessed in 24 plasma samples of healthy controls and 95 plasma samples of NSCLC patients. Reasonable results were obtained for four different genes; osteopontin and HIF-1α and two house-keeping genes, B2M and UBC.

No significant CA IX and CA XII expression was found to be detectable in blood plasma samples. It could be so that in order to detect tumor-derived mRNAs in plasma the tumors need to have active apoptosis and/or necrosis. Due to an absence of or only a small degree of apoptosis in tumors no CA IX and CA XII mRNA expression was found to be present in sufficient amounts to be detected in the plasma.

Majority of the investigated samples showed very low concentrations and only a few samples had high values. Therefore, it was challenging to perform qRT-PCR, and the obtained copy numbers were throughout low. These results would imply that the amounts of circulating nucleic acids are very low in plasma. For the osteopontin, the mRNA levels were extremely low for samples 1-56 although all the samples were

processed exactly in the same way. Because the results of the first 56 samples were considered unreliable, the statistical analysis was based on the 39 remaining samples.

6.1 Statistical analysis

Because it has been reported that the mRNA levels in the plasma of cancer patients are higher, it was assumed that the amount of the house-keeping genes is not constant throughout the samples. Therefore the difference in RNA levels between healthy controls and NSCLC patients were tested for the tumor-related genes as well as the house-keeping genes *B2M* and *UBC,* and the results of *OPN* and *HIF-1α* were analysed with and without the normalization to the house-keeping genes.

Our study showed that the mRNA levels in blood plasma were higher in the NSCLC patients than in the healthy controls. A statistically significant difference between these groups was found for *UBC* ($P = 0.001$), osteopontin ($P < 0.001$) and osteopontin normalized to housekeeping genes ($P < 0.001$). Based on these results the mRNA levels of *UBC* and osteopontin might have a diagnostic value. The mRNA levels were higher in the NCLC patients also for *HIF-1α* and *B2M*, but according to Wilcoxon Mann-Whitney test, these results were not statistically significant.

6.1.1 Correlation and survival analysis

The correlation between the mRNA levels and a number of tumor markers, as well as clinical characteristics was investigated. The tumor markers used in the correlation analysis were interleukin 6 and 8, CEA, CYFRA 21-1 and OPN. The majority of correlations between mRNA levels and blood tumor markers or clinical factors were not statistically significant. A strong statistically significant negative correlation was found between OPN mRNA and SUVmax, which is a maximum Standardized Uptake Value measured on PET scan. Unfortunately, SUVmax values were available only for 18 patients and a theoretical explanation for the found correlation is lacking.

The median follow-up of the NSCLC patients was 3.3 years (95% CI: 2.7-3.8 yr). The Cox regression analysis did not show any relationship between mRNA levels and survival of NSCLC patients. Therefore, these results suggest that the studied circulated mRNAs unlikely have a significant prognostic value in NSCLC patients.

6.1.2 ROC analysis

To evaluate the accuracy of the mRNA quantification, ROC analysis was performed. Receiver-operating characteristic (ROC) analysis is a useful tool for evaluating the performance of diagnostic tests that classifies subjects into 1 of 2 categories, diseased or nondiseased. The fundamental measures of diagnostic accuracy are sensitivity, i.e. true positive rate, and specificity, i.e. true negative rate. (Zou et al., 2007) In this study the ROC curve analysis was performed to examine whether the investigated genes would have potential as tumor markers.

A ROC curve is a plot of sensitivity versus 1-specificity, where the sensitivity is defined as the probability that a test gives a positive result in a subject with the disease. The specificity is defined as the probability that the test result is negative given the subject is truly non-diseased. Several summary indices are associated with the ROC curve. One of the most popular measures is the area under the ROC curve (AUC). AUC is a combined measure of sensitivity and specificity. It is a measure of the overall performance of a diagnostic test and is interpreted as the average value of sensitivity for all possible values of specificity. The larger the area under the curve, the better the diagnostic test would be. (Obuchowski, 2003) Since AUC is a measure of the overall performance of a diagnostic test, the overall diagnostic performance of different tests can be compared by comparing their AUCs. (Zou et al. 2007) If the AUC is 1.0, the sensitivity and specificity are both 100%. If the AUC is 0.5, the sensitivity and specificity are both 50%. In practice, a diagnostic test has an area somewhere between these two extremes. The closer the area is to 1.0, the better the test is, and the closer the area is to 0.5, the worse the test is. An AUC of <0.50 is considered worthless, 0.60–0.69 poor, 0.70–0.79 fair, 0.80–0.89 good and 0.90–1 excellent (Zhou et al. 2006).

In this study all of the AUC values of all the ROC curves were under 0.80. The ROC curve to *UBC* had the highest AUC value, 0.734. The sensitivity for lung cancer was 84.6% for *UBC,* 74.3% for *B2M*, 81.0% for the geometric mean of *UBC* and *B2M*, 78.4% for *OPN* and 65.2% for *HIF-1α*. The specificity for lung cancer was 62.1% for *UBC,* 49.8% for *B2M*, 55.0% for the geometric mean of *UBC* and *B2M*, 57.8% for *OPN* and 40.6% for *HIF-1α.*

The AUC values of the ROC analysis remained quite low compared to the requirements set for a diagnostic test. However, when evaluating the diagnostic performance of a test, it is also important to take into account the financial costs of the test and the risks and benefits the test has compared to other methods. After this it is possible to decide if the test is clinically usable.

7 Conclusions

Quantitative real-time polymerase chain reaction seemed to be challenging when analysing the mRNA levels of plasma samples because of the low amount of circulating RNA in plasma.

Based on this study, it is not possible to draw definitive conclusions. However statistically significant differences were found between certain mRNA levels of healthy controls and NSCLC patients. Therefore mRNA levels of *UBC* and osteopontin and osteopontin corrected with the house-keeping genes might have diagnostic value. The majority of correlations between mRNA levels and clinical parameters or blood biomarkers were not statistically significant. Neither did the survival analysis show any significant relationship between survival and mRNA levels. So the prognostic value of for the investigated genes seems to be very limited. According to the ROC curve analysis most of the investigated genes did not show potential as plasma tumor markers.

In conclusion, the sensitivity of molecular assays remains as the limiting step for a routine use of plasma biomarkers in clinical practice. It is possible that the combination of quantitative and qualitative molecular assays on plasma RNA, developed for high-throughput platforms, could improve the non-invasive approach to lung cancer detection.

REFERENCES

American Cancer Society. http://www.cancer.org/docroot/home/index.asp (06/09/2008).

Anker P, Lyautey J, Lederrey C, Stroum M. Circulating nucleic acids in plasma or serum. Clin Chim Acta 2001;313:143–146.

Bhattacharjee A, Richards WG, Staunton J, Li C, Monti S, Vasa P, Ladd C, Beheshti J, Bueno R, Gillette M, Loda M, Weber G, Mark EJ, Lander ES, Wong W, Johnson BE, Golub TR, Sugarbaker DJ, Meyerson M. Classification of human lung carcinomas by mRNA expression profiling reveals distinct adenocarcinoma subclasses. Proc Natl Acad Sci U S A. 2001;98:13790–5.

Bharti A, Ma PC, Salgia R. Biomarker discovery in lung cancer – promises and challenges of clinical proteomics. Mass Spectrometry Rev 2007;26:451–466.

Birner P, Schindl M, Obermair A, Plank C, Breitenecker G, Oberhuber G. Overexpression of Hypoxia-inducible Factor 1α Is a Marker for an Unfavorable Prognosis in Early-Stage Invasive Cervical Cancer. Cancer Res 2002;60:4693–4696.

Bogenrieder T, Herlyn M. Axis of evil: molecular mechanisms of cancer metastasis. Oncogene 2003 22:6524–36.

Brambilla E, Travis WD, Colby TV, Corrin B, Shimosato Y. The new World Health Organization classification of lung tumours. Eur Respir J 2001;18:1059–1068.

Bremnes RM, Sirera R, Camps C. Circulating tumour-derived DNA and RNA markers in blood: a tool for early detection, diagnostics, and follow-up? Lung Cancer 2005;49:1–12.

Breuer RHJ, Postmus PE, Smit EF. Molecular pathology of non-small-cell lung cancer. Respiration 2005;72:313–330.

Brown JM, Wilson WR. Exploiting tumour hypoxia in cancer treatment. Nature Rev Cancer 2004;4:437–447.

Chen HY, Yu SL, Chen CH, Chang GC, Chen CY, Yuan A, Cheng CL, Wang CH, Terng HJ, Kao SF, Chan WK, Li HN, Liu CC, Singh S, Chen WJ, Chen JJ, Yang PC. A five-gene signature and clinical outcome in non-small-cell lung cancer. N Engl J Med. 2007; 356:11–20.

Görlach A, Diebold I, Schini-Kerth VB, Berchner-Pfannschmidt U, Roth U, Brandes RP, Kietzmann T, Busse R. Thrombin activates the hypoxia-inducible factor-1 signalling pathway in vascular smooth muscle cells: Role of the p22(phox) containing NADPH oxidase. Circ Res. 2001;89:47–54.

Déry MAC, Michaud MD, Richard DE. Hypoxia-inducible factor 1: regulation by hypoxic and non-hypoxic activators. Int J Biochem Cell Biol 2005;37:535–540.

Donati V, Boldrini L, Dell'Omodarme M, Prati MC, Faviana P, Camacci T, Lucchi M, Mussi A, Santoro M, Basolo F, Fontanini G. Osteopontin expression and prognostic significance in non-small cell lung cancer. Clin Cancer Res 2005 11:6459–65.

Duarte RL, Paschoal MEM. Molecular markers in lung cancer: prognostic role and relationship to smoking. J Bras Pneumol 2005;32:56–65.

Esteller M, Sanchez-Cespedes M, Rosell R, Sidransky D, Baylin SB, Herman JG. Detection of aberrant promoter hypermethylation of tumor suppressor genes in serum DNA from non-small cell lung cancer patients. Cancer Res. 1999;59:67–70.

El-Hefnawy T, Raja S, Kelly L, Bigbee WL, Kirkwood JM, Luketich JD, Godfrey TE. Characterization of amplifiable, circulating RNA in plasma and its potential as a tool for cancer diagnostics. Clin Chem 2004;50:564–573.

Fedarko NS, Jain A, Karadag A, Van Eman MR, Fisher LW. Elevated serum bone sialoprotein and osteopontin in colon, breast, prostate, and lung cancer. Clin Cancer Res 2001;12:4060–6.

Giatromanolaki A, Koukourakis MI, Sivridis E, Pastorek J, Wykoff CC, Gatter KC, Harris AL. Expression of hypoxia-inducible carbonic anhydrase-9 relates to angiogenic pathways and independently to poor outcome in non-small cell lung cancer. Cancer Res 2001;61:7992–8.

Giulietti A, Overbergh L, Valckx D, Decallonne B, Bouillon R, Mathieu C. An overview of real-time quantitative PCR: applications to quantify cytokine gene expression. Mathods 2001;25:386–401.

Harris AL. Hypoxia – a key regulatory factor in tumour growth. Nature Rev Cancer 2002;2:38–47.

Hall WH. Ramachandran R. Narayan S. Jani AB. Vijayakumar S. An electronic application for rapidly calculating Charlson comorbidity score. BMC Cancer 2004;4:94.

Heighway J, Betticher DC. Lung tumors: an overview. Atlas Genet Cytogenet Oncol Haematol2004.http://AtlasGeneticsOncology.org/Tumors/LungTumOverviewID 5030.html (08/05/2008).

Hu Z, Lin D, Yuan J, Xiao T, Zhang H, Sun W, Han N, Ma Y, Di X, Gao M, Ma J, Zhang J, Cheng S, Gao Y. Overexpression of osteopontin is associated with more aggressive phenotypes in human non-small cell lung cancer. Clin Cancer Res 2005;11:4646–52.

Hynninen P, Vaskivuo L, Saarnio J, Haapasalo H, Kivelä J, Pastoreková S, Pastorek J, Waheed A, Sly WS, Puistola U, Parkkila S. Expression of transmembrane carbonic anhydrases IX and XII in ovarian tumours. Histopathology. 2006;49:594–602.

Hwang SM, Wilson PD, Laskin JD, Denhardt DT. Age and development-related changes in osteopontin and nitric oxide synthase mRNA levels in human kidney proximal tubule epithelial cells: contrasting responses to hypoxia and reoxygenation. J Cell Physiol 1994;160:61–8.

Höckel M, Vaupel P. Tumor hypoxia: definitions and current clinical, biologic, and molecular aspects. J Natl Cancer Inst 2001;93:266–76.

Ivanov SV, Kuzmin I, Wei MH, Pack S, Geil L, Johnson BE, Stanbridge EJ, Lerman MI. Down-regulation of transmembrane carbonic anhydrases in renal cell carcinoma cell lines by wild-type von Hippel-Lindau transgenes. Proc Natl Acad Sci U S A. 1998;95:12596–601.

Jemal A, Siegel R, Ward E, Hao Y, Xu J, Murray T, Thun MJ. Cancer statistics, 2008. CA Cancer J Clin 2008;58:71–96.

Ivanov S, Liao S, Ivanova A, Danilkovitch-Miagkova A, Tarasova N, Weirich G, Merrill MJ, Proescholdt MA, Oldfield EH, Lee J, Zavada J, Waheed A, Sly W, Lerman M, Stanbridge EJ. Expression of Hypoxia-inducible Cell-surface Transmembrane Carbonic Anhydrases in Human Cancer. Am J Pathol 2001 158:905–19.

Kim SJ, Rabbani ZN, Vollmer RT, Schreiber EG, Oosterwijk E, Dewhirst MW, Vujaskovic Z, Kelley MJ. Carbonic Anhydrase IX in Early-Stage Non-Small Cell Lung Cancer. Clin Cancer Res 2004;10:7925–7933.

Kivela AJ, Parkkila S, Saarnio J, Karttunen TJ, Kivela J, Parkkila AK, Bartosova M, Mucha V, Novak M, Waheed A, Sly WS, Rajaniemi H, Pastorekova S, Pastorek J. Expression of von Hippel-Lindau tumor suppressor and tumor-associated carbonic anhydrases IX and XII in normal and neoplastic colorectal mucosa. World J Gastroenterol 2005;11:2616–25.

Kubista M, Andrade JM, Bengtsson M, Forootan A, Jonák J, Lind K, Sindelka R, Sjöback R, Sjögreen B, Strömbom L, Ståhlberg A, Zoric N. The real-time polymerase chain reaction. Mol Aspects Med 2006;27:95–125.

Lang KJD, Kappel A, Goodall GJ. Hypoxia-inducible factor-1α mRNA contains an internal ribosome entry site that allows efficient translation during normoxia and hypoxia. Mol Biol Cell 2002;13:1792–1801.

Le QT, Chen E, Salim A, Cao H, Kong CS, Whyte R, Donington J, Cannon W, Wakelee H, Tibshirani R, Mitchell JD, Richardson D, O'Byrne KJ, Koong AC, Giaccia AJ. An evaluation of tumor oxygenation and gene expression in patients with early stage non-small cell lung cancers. Clin Cancer Res 2006;12:1507–1514.

Le QT, Sutphin PD, Raychaudhuri S, Yu SC, Terris DJ, Lin HS, Lum B, Pinto HA, Koong AC, Giaccia AJ. Identification of osteopontin as a prognostic plasma marker for head and neck squamous cell carcinomas. Clin Cancer Res 2003;9:59–67.

Leon SA, Shapiro B, Sklaroff DM, Yaros MJ. Free DNA in the serum of cancer patients and the effect of therapy. Cancer Res 1977 37:646–50.

Makino Y, Kanopka A, Wilson WJ, Tanaka H, Poellinger L, Inhibitory PAS domain protein (IPAS) is a hypoxia-inducible splicing variant of the hypoxia-inducible factor-3α locus. J Biol Chem 2002;277:32405–32408.

Manne U, Srivastava RG, Srivastava S. Keynote review: Recent advances in biomarkers for cancer diagnosis and treatment. DDT 2005;10:965–976.

Maxwell PH. The HIF pathway in cancer. Sem Cell Dev Biol 2005;16:523–530.

McKiernan JM, Buttyan R, Bander NH, Stifelman MD, Katz AE, Chen MW, Olsson CA, Sawczuk IS. Expression of the tumor-associated gene MN: a potential biomarker for human renal cell carcinoma. Cancer Res 1997;57:2362–2365.

Metzen E, Fandrey J, Jelkmann W. Evidence against a major role for Ca2+ in hypoxia-induced gene expression in human hepatoma cells (Hep3B). J Physiol 1999;15:651–7

Miura N, Nakamura H, Sato R, Tsukamoto T, Herada T, Takahashi S, Adachi Y, Shomori K, Sano A, Kishimoto Y, Ito H, Hasegawa J, Shiota G. Clinical usefulness of serum telomerase reverse transcriptase (*hTERT*) mRNA and epidermal growth factor receptor (*EGFR*) mRNA as a novel tumor marker for lung cancer. Cancer Sci 2006;97:1366–1373.

National Cancer Institute. http://www.cancer.gov/ (06/09/2008)

Niewoehner DE, Rubins JB. Clinical utility of tumor markers in the management of non-small cell lung cancer. Methods Mol Med 2003;75:135–141.

Nolan T, Hands RE, Bustin SA. Quantification of mRNA using real-time RT-PCR. Nat Protoc 2006;1:1559–82.

Oldberg A, Franzén A, Heinegård D. Cloning and sequence analysis of rat bone sialoprotein (osteopontin) cDNA reveals an Arg-Gly-Asp cell-binding sequence. Proc Natl Acad Sci U S A 1986;83:8819–23.

Obuchowski NA. Receiver operating characteristic curves and their use in radiology. Radiology 2003;229:3–8.

Pastorekova S, Parkkila S, Zavada J. Tumor-associated carbonic anhydrases and their clinical significance. Adv Clin Chem 2006;42:167–216.

Pastorekova S, Parkkila S, Pastorek J, Supuran CT. Carbonic anhydrases: current state of the art, therapeutic applications and future prospects. J Enzyme Inhib Med Chem 2004;19:199–229.

Quintero M, Mackenzie N, Brennan PA. Hypoxia-inducible factor 1 (HIF-1) in cancer. EJSO 2004;30:465–468.

Rangaswami H, Bulbule A, Kundu GC. Osteopontin: role in cell signaling and cancer progression. Trends Cell Biol 2006;16:79–87.

Richard DE, Berra E, Pouyssegur J. Non-hypoxic pathway mediates the induction of hypoxia-inducible factor 1 alpha in vascular smooth muscle cells. J Biol Chem 2000;275:26765–71.

Rittling SR, Chambers AF. Role of osteopontin in tumour progression. Br J Cancer 2004;90:1877–1881.

Rosell R, Felip E, Garcia-Campelo R, Balaña C. The biology of non-small-cell lung cancer:identifying new targets for rational therapy. Lung Cancer 2004;46:135–148.

Said HM, Hagemann C, Staab A, Stojic J, Kühnel S, Vince GH, Flentje M, Roosen K, Vordermark D. Expression patterns of the hypoxia-related genes osteopontin, CA9, erythropoietin, VEGF and HIF-1alpha in human glioma in vitro and in vivo. Radiother Oncol 2007;83:398–405.

Sánchez-Céspedes M, Monzó M, Rosell R, Pifarré A, Calvo R, López-Cabrerizo MP, Astudillo J. Detection of chromosome 3p alterations in serum DNA of non-small-cell lung cancer patients. Ann Oncol 1998;9:113–6.

Schindl M, Schoppmann SF, Samonigg H, Hausmaninger WK, Gnat M, Jakesz R, Kubitsa E, Birner P. Overexpression of hypoxia-inducible factor 1α is associated with an unfavorable prognosis in lymph node-positive breast cancer. Clin Cancer Res 2002; 8:1831–1837.

Semenza GL, Wang GL. A nuclear factor induced by hypoxia via de novo protein synthesis binds to the human erythropoietin gene enhancer at a site required for transcriptional activation. Mol Cell Biol 1992;12:5447–5454

Semenza GL. Targeting HIF-1 for cancer therapy. Nature Rev Cancer 2003;3:721–732.

Semenza GL. Hypoxia-inducible factor 1 (HIF-1) pathway. Sci STKE 2007;407.

Simi L, Venturini G, Malentacchi F, Gelmini S, Andreani M, Janni A, Pastorekova S, Supuran CT, Pazzagli M, Orlando C. Quantitative analysis of carbonic anhydrase IX mRNA in human non-small cell lung cancer. Lung Cancer 2006;52:59–66.

Sisco KL. Is RNA in serum bound to nucleoprotein complexes? Clin Chem. 2001;47:1744–5.

Strauss GM, Skarin AT. Use of tumor markers in lung cancer. Hematol Oncol Clin North Am 1994;8:507–532.

Sulzbacher I, Birner P, Trieb K, Lang S, Chott A. Expression of osteopontin and vascular endothelial growth factor in benign and malignant bone tumors. Virchows Arch 2002;441:345–9.

Svastová E, Hulíková A, Rafajová M, Zat'ovicová M, Gibadulinová A, Casini A, Cecchi A, Scozzafava A, Supuran CT, Pastorek J, Pastoreková S. Hypoxia activates the capacity of tumor-associated carbonic anhydrase IX to acidify extracellular pH. FEBS Lett. 2004;577:439–45.

Swinson DEB, Jones JL, Cox G, Richardson D, Harris AL, O'Bryne KJ. Hypoxia-inducible factor-1α in non small cell lung cancer: relation to growth factor, protease and apoptosis pathways. Int J. Cancer 2004;111:43–50.

Thalmann GN, Sikes RA, Devoll RE, Kiefer JA, Markwalder R, Klima I, Farach-Carson CM, Studer UE, Chung LW. Osteopontin: possible role in prostate cancer progression. Clin Cancer Res 1999;8:2271–7.

Thomlinson RH, Gray LH. The histological structure of some human lung cancers and the possible implications for radiotherapy. Br J Cancer 1955;4:539–49.

Tong YK, Lo YMD. Diagnostic developments involvilg cell-free (circulating) nucleic acids. Clin Chim Acta 2006;363:187–196.

Tuck AB, Chambers AF. The role of osteopontin in breast cancer: clinical and experimental studies. J Mammary Gland Biol Neoplasia 2001;4:419–29.

Türeci O, Sahin U, Vollmar E, Siemer S, Göttert E, Seitz G, Parkkila AK, Shah GN, Grubb JH, Pfreundschuh M, Sly WS. Human carbonic anhydrase XII: cDNA cloning, expression, and chromosomal localization of a carbonic anhydrase gene that is overexpressed in some renal cell cancers. Proc Natl Acad Sci U.S.A 1998;95:7608–13.

Vaupel P. The role of hypoxia-induced factors in tumor progression. Oncologist 2004;9:10–17.

Vaupel P, Mayer A. Hypoxia in cancer: significance and impact on clinical outcome. Cancer Metastasis Rev 2007;26:225–239.

Wang GL, Jiang BH, Rue EA, Semenza GL. Hypoxia-inducible factor 1 is a basic-helix-loop-helix-PAS heterodimer regulated by cellular O_2 tension. Proc. Natl. Acad. Sci. U.S.A 1995;92:5510–5514.

Weber GF. The metastasis gene osteopontin: a candidate target for cancer therapy. Biochim Biophys Acta. 2001;1552:61–85.

Wong ML, Medrano JF. Real-time PCR for mRNA quantitation. Biotechniques 2005;39:75–85.

Wouters BG, van den Beucken T, Magagnin MG, Koritzinsky M, Fels D, Koumenis C. Control of hypoxic response through regulation of mRNA translation. Sem Cell Dev Biol 2005;16:487–501.

Wouters BG, van den Beucken T, Magagnin MG, Lambin P, Koumenis C. Targeting hypoxia tolerance in cancer. Drug Resistance Updates 2004;7:25–40.

Wykoff CC, Beasley N, Watson PH, Turner KJ, Pastorek J, Sibtain A, Wilson GD, Turley H, Talks KL, Maxwell PH, Pugh CW, Ratcliffe PJ, Harris AL. Hypoxia-inducible Expression of tumor-associated Carbonic Anhydrases. Cancer Res 2000;60:7075–7083.

Závada J, Závadová Z, Pastoreková S, Ciampor F, Pastorek J, Zelník V. Expression of MaTu-MN protein in human tumor cultures and in clinical specimens. Int J Cancer 1993;54:268–274.

Zhang J, Takahashi K, Takahashi F, Shimizu K, Ohshita F, Kameda Y, Maeda K, Nishio K, Fukuchi Y. Differential osteopontin expression in lung cancer. Cancer lett 2001;171:215–22.

Zhou Y, Dai DL, Martinka M, Su M, Zhang Y, Campos EI, Dorocicz I, Tang L, Huntsman D, Nelson C, Ho V, Li G. Osteopontin expression correlates with melanoma invasion. J Invest Dermatol. 2005;124:1044–52.

Zhou W, Li H, Gu Y, Yu L, Han J, Xu W, Jian W, Tian J, Zhou W, Zhang D, Liu Y, Yang J, Li J, Li G, Luo M. The ROC analysis for different time points during oral glucose tolerance test. Diabetes Res Clin Pract. 2006;72:88–92.

Zou KH. O'Malley J. Mauri L. Receiver-Operating Characteristic Analysis for Evaluating Diagnostic Tests and Predictive Models. Circulation 2007;115:654–7.

Zhu Y, Denhart DT, Cao H, Sutphin PD, Koong AC, Giaccia AJ, Le QT. Hypoxia upregulates osteopontin expression in NIH-3T3 cells via a *Ras*-activated enhancer. Oncogene 2005;24:6555–6563.